MAX-PLANCK-GESELLSCHAFT

Diploma Thesis

In vivo visualization of inhibitory odor responses in the olfactory system of the fruit fly *Drosophila melanogaster*

accomplished at the

Max Planck Institute for Chemical Ecology

submitted by

Veit Grabe

[February/22/2010]

First Reviewer: Prof. Dr. Bill Hansson

Second Reviewer: PD Dr. Dieter Wicher

Table of Contents

1. Introduction

The main goal of this work was the analysis of inhibitory responses induced by odors in the olfactory system of *Drosophila melanogaster*. Although the system is very profoundly examined in regard to its excitatory functions only few studies were dedicated to the role of inhibitory neural circuits. Researchers agree on the existence of an inhibitory contribution to the processing of olfactory information since there is more and more evidence like the GABAergic local interneurons (LNs) (WILSON & LAURENT, 2005) or the observations on more complex processing functions with incontestable inhibitory input (OKADA et al., 2009; OLSEN & WILSON, 2008). Regarding any behavioral relevance, it has been shown that a knockdown of $GABA_B$-type receptors in olfactory sensory neurons (OSN), i.e. blocking the inhibitory input in these neurons, result in an impairment of the localization of odor sources (ROOT et al., 2008).

To examine the inhibitory tasks in *Drosophila in vivo* I used a relatively newly developed transgenic, ratiometric sensor called clomeleon which is chloride sensitive (KUNER & AUGUSTINE, 2000). Since chloride ions are the main mediator of inhibitions in mature neurons, this sensor enables to visualize inhibitory neural responses. Clomeleon has been successfully used in mice to analyze the inhibitory tasks in the hippocampus (BERGLUND et al., 2006; POND et al., 2006), the cerebellum and the amygdala *in vitro* (BERGLUND et al., 2008) and in the retina *in vivo* (DUEBEL et al., 2006; HAVERKAMP, et al., 2005; WÄSSLE et al., 2009). So far clomeleon has never been used to study inhibitions in the olfactory system nor has it been applied for *Drosophila*. With the help of this new sensor and the already established calcium reporter, cameleon (MIYAWAKI et al. 1997), I was able to image inhibitory as well as excitatory responses in OSNs on the antenna and in the first processing center of *Drosophila melanogaster*, the antennal lobe. In addition I performed imaging of odor-induced responses in projection neurons (PNs) under the same conditions in the antennal lobe. I verified some basics of the inhibitory pathway at the input and output level to approach a more complete knowledge of the whole olfactory reception network.

1.1. The sense of Olfaction

Olfaction plays a major role in the life of *Drosophila melanogaster* and as a special form of chemoreception in the life of most other prokaryotes and eukaryotes since millions of years. Its importance is known in essential tasks like to seek and judge potential food sources, find mating partners, search proper places to oviposit and prevent encountering predators. From the simple single cellular structures in early metazoans over the more complex organs in annelids and early arthropods to the highly derived appendages and associated neural structures in insects and mammals the perception, transmission and transduction of chemical cues was crucial for survival (SCHMIDT-RHAESA, 2007). One of the specialized expansions of chemoreceptive senses is olfaction which is remarkably similar evolved in vertebrates and insects (HILDEBRAND & SHEPERD, 1997; EISTHEN, 2002) and is capable to perceive and discriminate an exceptional number of odors although its morphology is differentially distinct in both taxa.

1.2. *Drosophila melanogaster* as a model system

Since the whole genome of *Drosophila melanogaster* has been sequenced (ADAMS et al., 2000), although it is not the only one anymore, it is still favored as one of the most common genetic model organisms. Due to the fact that scientists used to work with the fruit fly for about 100 years (CASTLE, 1906) it became the number one tool for examining behavioral, physiological and genetic basics. Furthermore the short generation time, modest diet as well as their already well examined behavior and general biology marks them as unequally good research objects in addition to the advantage of an enormous international community of scientists in almost every biological field.

Over the past years *Drosophila melanogaster* became a popular model organism to analyze a reduced olfactory system. In contrast to the complex vertebrate olfactory system the *Drosophila* one is extremely reduced consisting of about 60 olfactory receptors (ORs). The mouse possesses about 1000 OR genes (BUCK & AXEL, 1991). The simplification makes it very comfortable to examine and decipher basic mechanisms of odor perception in the fruit fly's olfactory system. However, the two systems resemble each other in basic structure and connectivity making it possible to compare fundamental neuronal functionalities. Another

advantage which comes with the decoding of the genome is the availability of the GAL4:UAS system (BRAND & PERRIMON, 1993; Figure 1) and a lot of other genetic techniques allowing me to measure specific neuronal populations. This circumstance emphasizes the work with *Drosophila* compared to other arthropod species which do not offer such a genetic toolbox. The mentioned system is a genetic tool derived from the yeast *Saccharomyces cerevisiae* where it is responsible for the activation of genes triggered by the presence of galactose. In genetics this system is used to express various proteins only in special regions by the usage of a tissue specific driver. This driver is combined with the GAL4-sequence so that in case of expression of the driver in the targeted tissue also GAL4 is expressed. In *Saccharomyces cerevisiae* the GAL4 binds to a so-called upstream activating sequence (UAS) which triggers the expression of a gene lying downstream. The system was established for *Drosophila* to target gene expression in specific cells (BRAND & PERRIMON, 1993). In *Drosophila melanogaster* the UAS can be combined with almost any protein sequence but in my diploma thesis I used the calcium or chloride sensitive sensors cameleon or clomeleon.

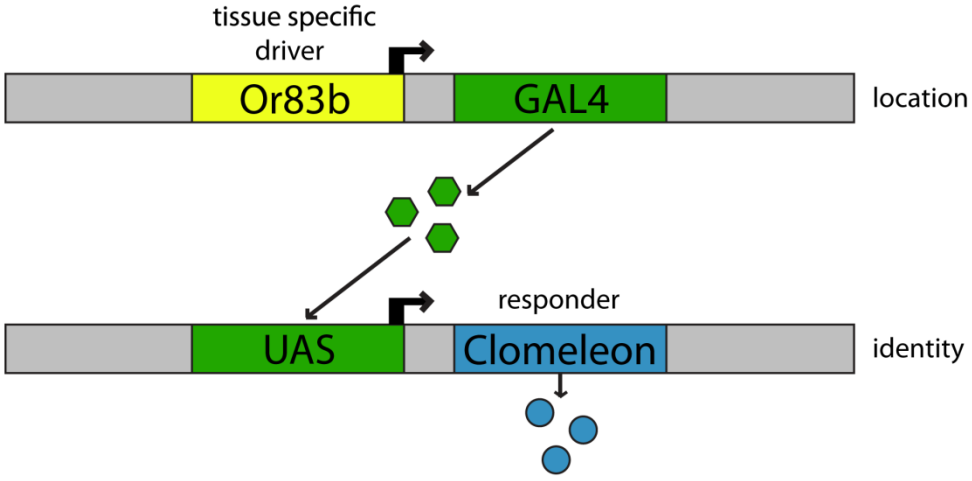

Figure 1. The GAL4:UAS system.
The tissue specific driver OR83b initiates the expression of the inserted GAL4 sequence in a large population of OSNs. The expressed GAL4 then binds to the upstream activating sequence (UAS) present in the same cells which then leads to the expression of the responder, the chloride sensitive sensor clomeleon in this case.

1.3. The olfactory system of *Drosophila*

The olfactory system of *Drosophila* is on a similar functional level as in vertebrates (MOMBAERTS, 1999; EISTHEN, 2002; BARGMANN, 2006). The gate to the system is placed on the third antennal segment, the so-called funiculus, where the sensillae are located (Figure 2B left). These morphological units are separated in three subtypes which are the so-called coeloconic, trichoid and basiconic sensilla. The latter can be split into large and small basiconic ones (SHANBHAG et al., 1999). Depending on their type the different sensillae are relevant to percept food odors, pheromones or CO_2 (VOSSHALL& STOCKER, 2007). Within these bristles OSNs are housed in numbers of one to four (de BRUYNE et al., 2001; COUTO et al., 2005). Additional to the neurons in the maxillary palps, the circa 1200 OSNs (STOCKER, 1994) in each antenna express one certain OR out of the almost 40 ORs that are expressed in adults which belong to approximately 62 known ORs in total in *Drosophila* (VOSSHALL et al, 2000). They are transcribed from 60 genes whereas two ORs arise through alternative RNA splicing (ROBERTSON et al., 2003). Each of the OSNs expresses only one conventional OR (CLYNE et al., 1999) together with OR83b, a co-receptor essential for the perception of odorants (LARSSONet al., 2004) as well as for the expression of the conventional receptors in the right compartments (BENTON et al., 2006). Additional there are several neurons expressing two conventional ORs (GOLDMAN et al., 2005). In general about 30 neurons form a population of OSNs expressing one specific OR and send their axons towards the protocerebrum where they converge to discrete spherical, functional units so-called olfactory glomeruli (GAOet al., 2000; VOSSHALL et al., 2000; Figure 2B middle). Corresponding to the number of ORs each antennal lobe should consist of approximately 40 glomeruli. However, some OSN populations innervate also a second glomerulus (FISHILEVICH et al., 2005). Within the antennal lobes the LNs connect different OSNs with each other to diversify the sensory input from the antenna. Since there are cholinergic as well as GABAergic LNs (WILSON & LAURENT, 2005; SHANG et al., 2007), they execute excitatory as well as inhibitory tasks and are capable of broadening and/or narrowing the olfactory input signal.

Next to the OSNs the main target of the LNs are the PNs, second order neurons which gather the olfactory information in the antennal lobe and guide it to higher brain centers like the mushroom body calyx and the lateral protocerebrum, also called lateral horn (STOCKER et al., 1990). On their way to the higher brain centers the PN axons form so-called

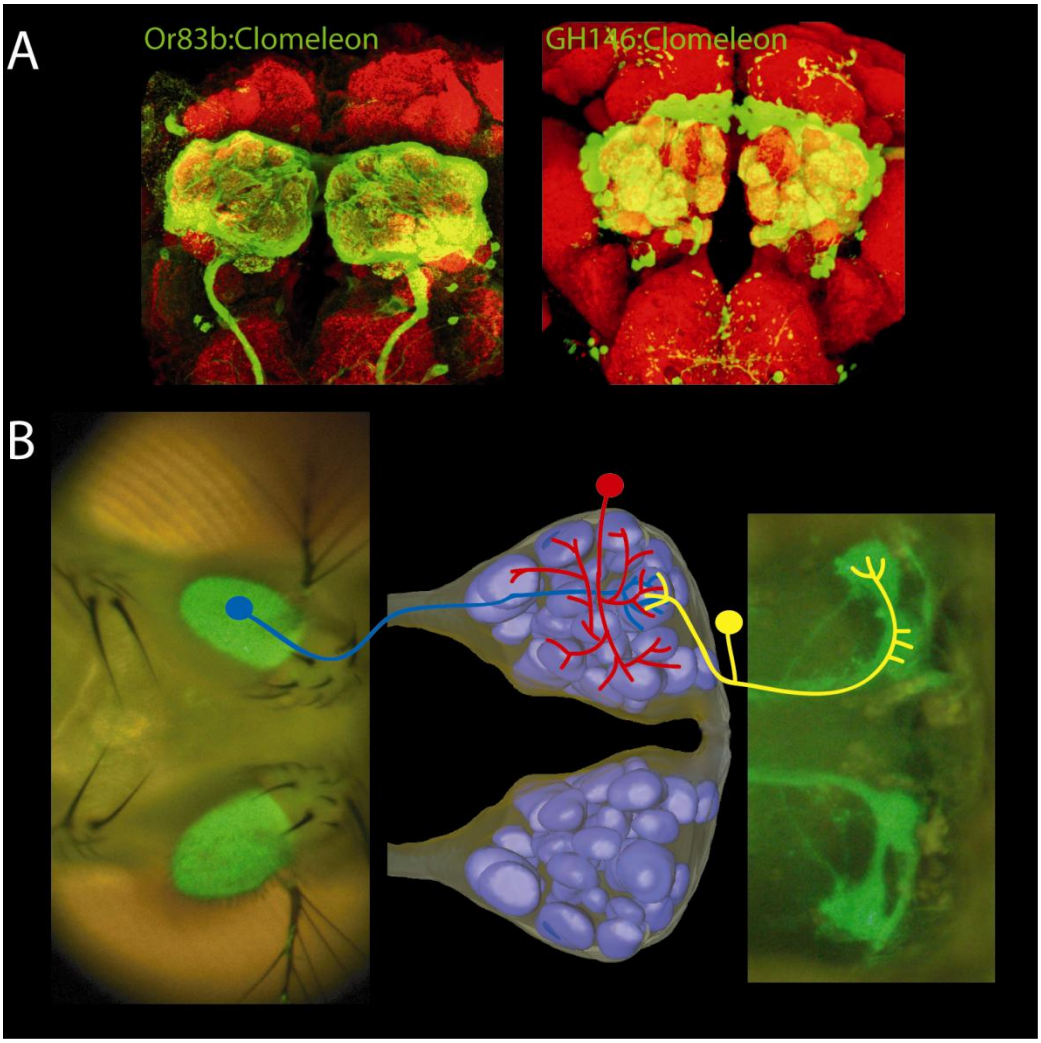

Figure 2. Schematic depiction of the *Drosophila* olfactory system.
(A) Projections of confocal stacks generated from immunostained extracted brains (α-nc82/α-GFP). **(B)** Fluorescence images of the antennae (OR83b;clomeleon) and the mushroom bodies (GH146;clomeleon) connected via a 3D-reconstruction of the antennal lobe glomeruli created based on the OR83b-GAL4:UAS-clomeleon line (blue = OSN, red = LN, yellow = PN).

antennoprotocerebral tracts (APTs) classified in the medial (mAPT) and mediolateral APT (mlAPT) which are shown in Figure 2B (right). The lateral tract (lAPT) is not included in the used GH146 line which is a specific GAL4 line labeling a diverse set of PNs. The PNs are split in three distinct populations. With regard to the localization of their cell bodies arranged around the antennal lobe, they form the anterodorsal, lateral and ventral cell cluster (JEFFERIS et al., 2001; BERDNIK et al., 2008). Most of these PNs are cholinergic except the ones forming the mlAPT which are known to be GABAergic (OKADA et al., 2009). Summing up the glomerulus as a functional unit contains three neuronal classes: The axons of OSNs, the dendrites of PNs and the neurites from LNs that interconnect the different glomeruli

(STOCKER et al., 1990). At the next processing level, the target neuropiles of the PNs, the major processing of the olfactory information takes place integrating it with the input from the optical, gustatory and mechanosensory system to perform a broad integration of all senses. Sensory neurons that express gustatory receptors (GRs) originate from the maxillary palps and project to the suboesophageal ganglion (SOG). Via interneurons it is possible that their input is forwarded to the mushroom bodies (SINAKEVITCH & STRAUSFELD, 2006).

Although the second order neuropiles accomplish the main processing of information already at the level of the antennal lobe lots of processing is taking place. As mentioned above the LNs are connecting the first order OSNs with each other and with the second order PNs horizontally to build a network within the antennal lobe. Long time only the excitatory tasks of this system were studied in research but since the relevance of GABA has been shown (NG et al., 2002) and the existence of GABAergic LNs was revealed (WILSON et al., 2005) it is obvious that lateral input can be inhibitory as well. At the moment the LNs are the major origin of GABAergic inhibition throughout the antennal lobe since OSNs as well as PNs only form excitatory synapses and express choline acetyltransferase (PYTHON & STOCKER, 2002; WILSON et al., 2004b). Only some PNs from the ventral cluster seem to be GABA-immune-positive as well (WILSON & LAURENT, 2005; ITO et al., 1997).

1.4. The role of inhibition and GABA

The role of inhibition in processing was neglected for a long time in neurophysiology and most other research fields. Due to the fact that the majority of accessible methods are related to excitation and calcium currents it is no wonder. But the existence of GABAergic LNs in addition to the cholinergic ones (WILSON et al., 2005) shows that the physiological basis for a relevant inhibitory lateral input is given. Analysis of this phenomenon remained difficult without adequate dyes or transgenic sensors. Luckily in 2000, Kuner and Augustine developed clomeleon (KUNER & AUGUSTINE, 2000), a chloride sensitive sensor which works similar as the well known cameleon (MIYAWAKI et al., 1997), a calcium sensitive reporter. With this transgenic tool the possibilities of examining the modulatory pathways in the fly's brain are doubled. GABA is responsible for the main part of the measured chloride responses as it is known as the main neurotransmitter of inhibition in the central nervous system of invertebrates. GABAergic neurons can be LNs and some PNs of the mlAPT (OKADA et al.,

2009). This suggests different pathways of lateral inhibition (Figure 3). The LNs can interconnect two OSNs belonging to different or the same glomerulus (Figure 3A), they can guide inhibitory input from one OSN to a PN in another glomerulus or the other way around (Figure 3B) and they can connect OSNs with PNs within a single glomerulus (Figure 3C). The PNs are more restricted regarding their inhibitory input within the antennal lobe. So far they can only interconnect with each other in a single glomerulus (Figure 3D). The major part of their GABAergic input happens in the lateral horn (OKADA et al., 2009). To acquire significant data regarding these mechanisms it is essential to measure the chloride signals in a comparable manner together with excitatory neural responses since GABAergic LNs and PNs first of all receive excitatory input before generating a lateral inhibition.

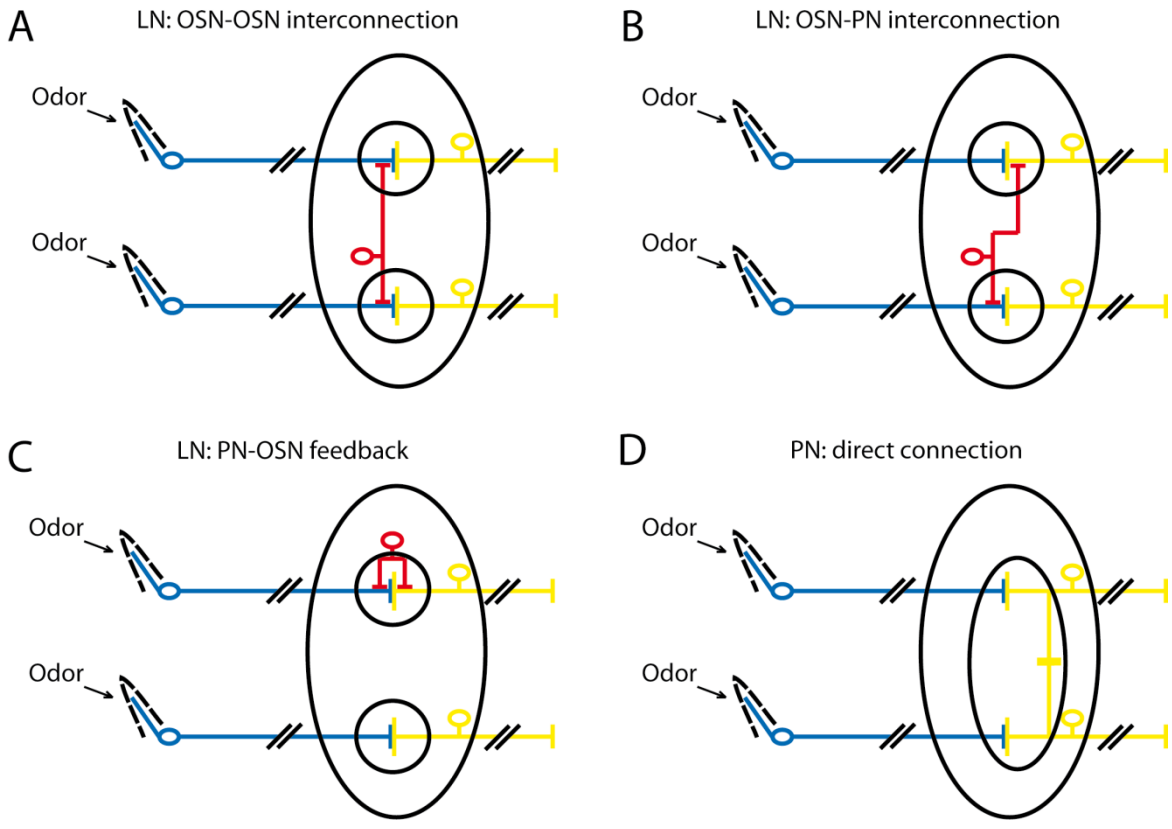

Figure 3. The mechanisms of lateral excitatory and inhibitory input in the antennal lobe of *Drosophila melanogaster*.
(A) An interglomerular feedback loop from a PN to the according presynaptic OSN via a LN. **(B)** A LN connecting two OSNs in different glomeruli with dissimilar input. **(C)** A LN connects an OSN with a PN in another glomerulus. **(D)** The direct connection of two PNs within a single glomerulus. (blue = OSN, red = LN, yellow = PN)

1.5. OR22a

I chose the olfactory receptor 22a (OR22a) to study the inhibitory odor responses in OSNs in detail. OR22a has been well described regarding its excitatory functionality (PELZ et al., 2006) and therefore delivers a good basis for comparison with my inhibitory data. The chosen receptor 22a is known to percept general food odors and is expressed in neurons housed in a set of large basiconic sensillae on the antenna (DOBRITSA et al., 2003; Figure 4A). These are located on the ventral side of the antenna in an enclosed posterior area on the third antennal segment which is the first flagellum segment (VOSSHALL et al., 2000; FISHILEVICH et al., 2005; Figure 4B). As already described, the neuronal population expressing OR22a converges to a single spherical structure within the antennal lobe targeting the glomerulus DM2 (Figure 4C). The abbreviation means “dorsal median” number 2, since this glomerulus lies on the dorso-medial margin of the antennal lobe. Since it is not the only one in this region every single glomerulus has a number for identification (LAISSUE et al., 1999). The OR22a expressing neuron has been well characterized regarding its electrophysiological spiking pattern and odor responses (de BRUYNE et al., 2001; DOBRITSA et al., 2003; STENSMYR et al., 2003; HALLEM et al., 2004; HALLEM& CARLSON, 2006). Further its molecular receptive range is characterized in detail (PELZ et al., 2006) meaning the spectrum of olfactory ligands. This includes the binding characteristic of the ligands (HALLEM et al., 2004) as well as the associated olfactory binding proteins (OBPs) that interact with the ligands and the receptor (POPHOF, 2004), the OSNs housed in the same sensillum (DOBRITSA et al., 2003), co-receptors (DOBRITSA et al., 2003; LARSSON et al., 2004; NEUHAUS et al., 2005; BENTON et al., 2006) and G-proteins (SHIROKOVA, et al., 2005).

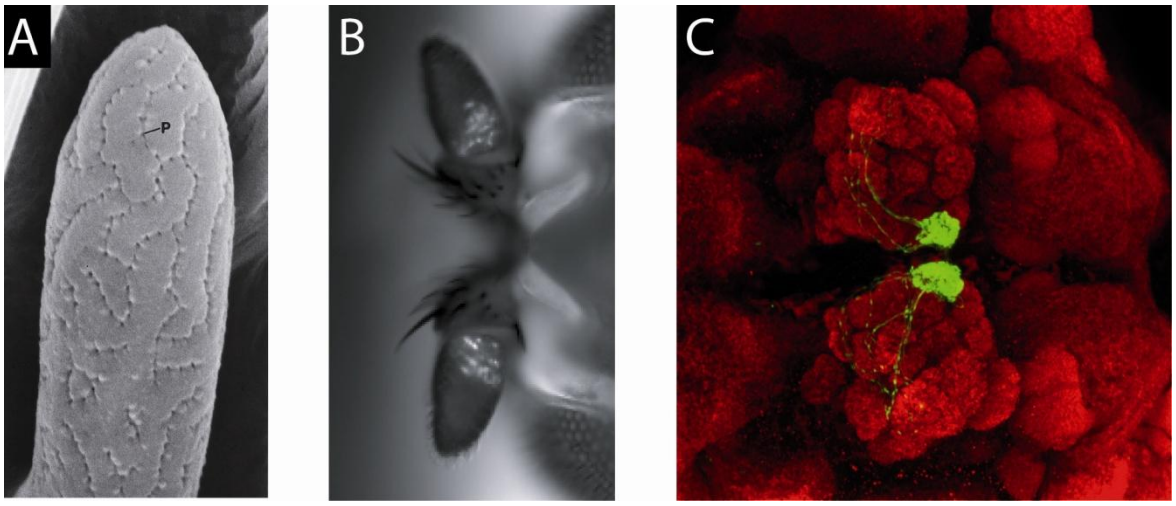

Figure 4. Morphology of the OR22a-GAL4:UAS-clomeleon line.
(A) High resolution scanning electron micrograph of a large basiconic sensilla (P = pore) (SHANBHAG et al., 1999). **(B)** View on the posterior side of the funiculus (third antennal segment) with the labeled OSN cell bodies expressing clomeleon. **(C)** View from anterodorsal on the immunostained fly brain with the OR22a expressing OSNs targeting the DM2 glomerulus (green, α-GFP) and the surrounding neuropil (red, α-nc82).

1.6. Goals of this work

My aim of this thesis is to characterize the odor induced inhibitory signals in the olfactory system of *Drosophila* and to compare them with the according excitation. Using the olfactory receptor OR22a as an example, I will show that, with the help of clomeleon, the possibilities to examine the olfactory code are doubled giving me a whole new point of view on the processing level of olfaction. Inhibition was often neglected and just mentioned as a marginal note to the expected major role of excitation in neurophysiology. With new, chloride sensitive, tools it is now possible to revise this opinion.

The main goals of my diploma thesis are as follows:

- Introducing clomeleon as a functional chloride indicator for the olfactory system of *Drosophila melanogaster*.

- Examining the inhibitory pathways throughout the first olfactory processing center of *Drosophila*, the antennal lobe.

- Analyzing modulatory mechanisms within the antennal lobe induced by the application of specific odors.

2. Material & Methods

2.1. Fly lines& breeding

The specimens of *Drosophila melanogaster* utilized for this research were aged between 3 and 15 days. The breeding of the single lines was done in an incubator at 25°C and 70% humidity with 12 hours day and night cycle. Every two weeks the flies were flipped into a new vial with food. 1 liter of this special fly food consisted of 918ml water, 95g polenta, 11g brewer's yeast, 2,4ml propionic acid, 3,3ml nipagine (16%), 118g sugar beet molasses and 4,1g agarose. For my experiments I used several transgenic fly strains modified with the help of the GAL4:UAS system (see Introduction). These flies expressed one of the two proteins cameleon or clomeleon in distinct neuronal populations making it easier to assign signals to the right neuronal pathway. We used five different transgenic fly lines, three GAL4 lines and two UAS lines. The GAL4 lines were OR22a (VOSSHALL et al., 2000), OR83b and GH146 (STOCKER et al., 1997). Additional UAS lines were cameleon2.1 (FIALA et al., 2002) and clomeleon (SACHSE unpublished). The five resulting different crossbreeds that I used for my experiments are listed in Table 1.

The GAL4 lines needed for the specific expression are commercially available at the Bloomington stock center but the UAS-lines with the corresponding genes have been generated by André Fiala (UAS-cameleon) and Silke Sachse (UAS-clomeleon).

Table 1. List of the used transgenic fly lines.

Fly line	Expressing neurons	Source
OR83b-GAL4:UAS-Cam	Nearly all OSNs	Fiala
OR83b-GAL4:UAS-Clom	Nearly all OSNs	Vosshall/ Sachse
OR22a-GAL4:UAS-Cam	OR22a expressing OSNs	Pelz
OR22a-GAL4:UAS-Clom	OR22a expressing OSNs	Vosshall/ Sachse
GH146-GAL4:UAS-Clom	A large subset of PNs	Vosshall/ Sachse

2.2. Antennal lobe and antenna dissection

Preparing the flies for the dissection I separated them in smaller vials and put them on ice for at least about 15 minutes to anesthetize them. After that one can grab them at the wing basis and fix them in a custom made stage (Figure 5A). The stage is a plastic block with one beveled side and a tiny copperplate (Athene Grids ©) glued to the upper edge of the bevel. In this plate there is a 125 µm slit which is just wide enough to fit around the neck of the fly. To prevent the fly from slipping out of the slit, I fixed the head with a minutia needle (Austerlitz, Insect Pins ©), glued to the stage with dental wax (Deiberit, Dr. Böhme and Schöps Dental GmbH). To melt the wax I used a soldering-iron (Voltcraft, PS152A). To minimize the movement artifacts during the measurement and to ease the cutting of the head capsule, the back of the head is glued to the stage with kollophonium (Royal Oak, Rosinio), solved in 99% ethanol. After it dried for 30 minutes a wire plate is placed on the bevel side of the stage with a thin wire behind the antenna and pushed in the flexible area between their basis and the remaining head capsule. Fixed with wax it is possible to bend the plate and with it the antennae forward by screwing two integrated screws on the left and right side of the fly.

The vertex is now good to see and cut, but before that the window plate is attached on top of the stage with the windows margin directly lying behind the antenna so that the antennae are sited underneath the plate and the vertex can still be seen. Finally the margin has to be sealed with a two-component silicone (Kwik-Sil, WPI) to prevent the saline from running through. Now after applying the saline (130mM NaCl, 5mM KCl, 2mM MgCl(*6H_2O), 2mM $CaCl_2$(*2H_2O), 36mM Saccharose, 5mM Hepes, pH 7.3 (ESTES et al., 1996)) the vertex is cut through the eye margins, the ocelli and behind the basis of the antenna to create a window which can be opened. Remaining fatty, tracheal and glandular tissue has to be removed with fine forceps (F.S.T., No. 11252-00) and the antennal lobes were accessible for the following imaging measurements.

Regarding the imaging of the antenna, the dissection was more simplified. The dissection consisted just of fixing the fly in the stage with a minutia needle and gluing the arista either to the eye, to have a good view on the anterior side of the funiculus, or to the vertex, erecting the funiculus to see the posterior funicular side. With the anterior perspective it was possible to image the three different sensillar regions of the funiculus, visible in the

OR83b lines, and to get an overview on the general spatiotemporal signal pattern evoked by odorants on the whole antenna. The posterior view was required to see the dendrites of the OR22a expressing neurons housed in the ab3 sensillae which are all located on the posterior basis of the funiculus (FISHILEVICH& VOSSHALL, 2005; de BRUYNEet al., 2001).

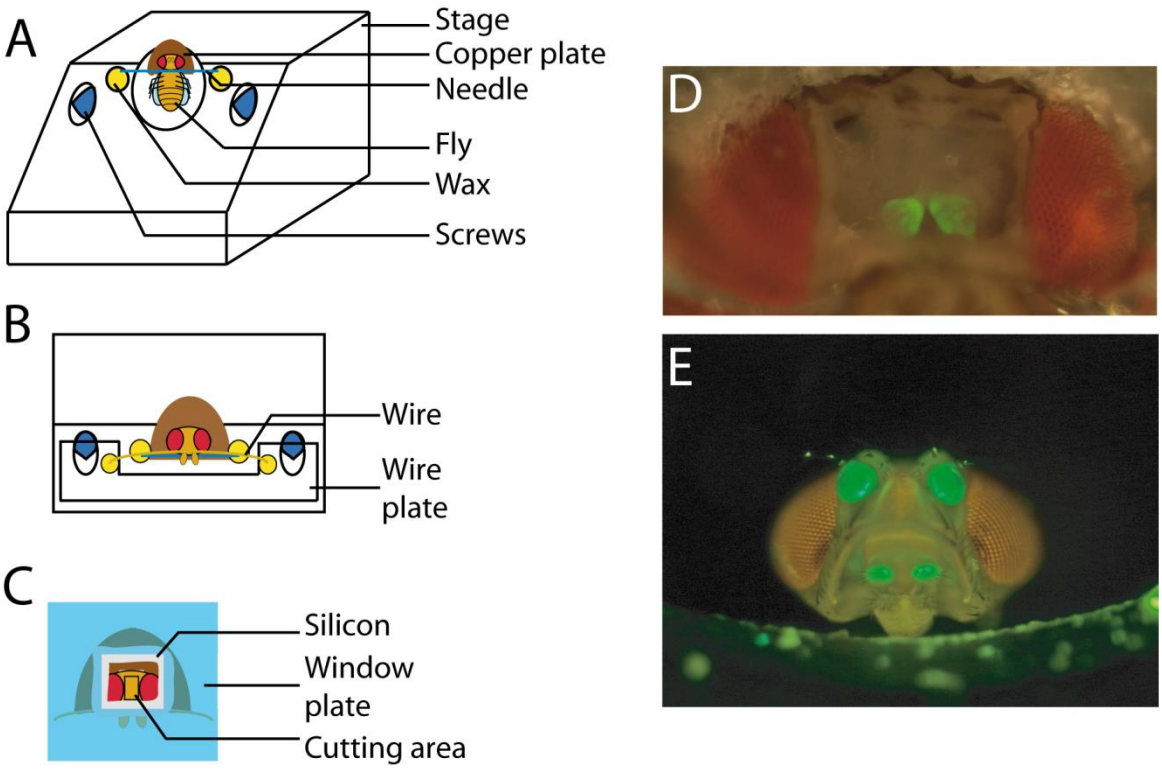

Figure 5. Dissection steps and setup.
(A) A fixed fly in the custom made dissection stage seen from frontal. **(B)** The dorsal view onto the fly with the attached wire to bend the antennae. **(C)** A dorsal view with the applied and sealed window plate. **(D)** A morphological view inside the head capsule from dorsal after the vertex has been removed as well as the fatty and tracheal tissues beneath. **(E)** Morphological image from anterior on the head of an OR83b-GAL4:UAS-clomeleon fly with the fluorescence microscope.

2.3. The sensors (clomeleon & cameleon)

Clomeleon is a genetically engineered chloride sensitive reporter developed by KUNER & AUGUSTINE in 2000 (KUNER & AUGUSTINE, 2000). It consists of an enhanced cyan fluorescent protein (eCFP) and an enhanced yellow fluorescent protein (eYFP) fused via a peptide linker. The excitation wavelength is 434nm to excite the eCFP, while the eYFP is excited by fluorescence resonance electron transfer (FRET) from the CFP to the YFP which leads to an

YFP emission wavelength of 527nm. When the transgenic clomeleon is expressed in specific target neurons with the help of the GAL4:UAS system and these neurons undergo an influx of chloride ions, these ions will bind to the receptive site of the eYFP and block the FRET effect. In that case the emitting photons will change their wavelength from 527nm to 485nm which is the normal emission wavelength of eCFP. Since clomeleon is a ratiometric sensor I divided the fluorescent changes recorded for both fluorescent proteins and calculated a ratio. This ratio gives the intracellular change in chloride concentration all over the antennal lobe as well as in specific neuronal areas dependent on the GAL4-line that has been used. With this information I could assign the application of several odors with a specific spatiotemporal inhibitory pattern in the antennal lobe.

The mechanism of cameleon is quite similar to clomeleon but the other way around. It was developed by MIYAWAKI and colleagues (MIYAWAKI et al., 1997) to measure localized Ca^{2+} currents in the cytosol. Cameleon also consists of an eCFP and an eYFP but this time the two proteins are connected via a calmodulin and a M13 domain which binds the calmodulin. If the intracellular Ca^{2+} concentration rises due to a Ca^{2+} influx, probably mediating an excitatory input, Ca^{2+} binds to the calmodulin which leads to a conformational change and brings the eCFP and eYFP closer together to amplify the FRET between the two proteins.

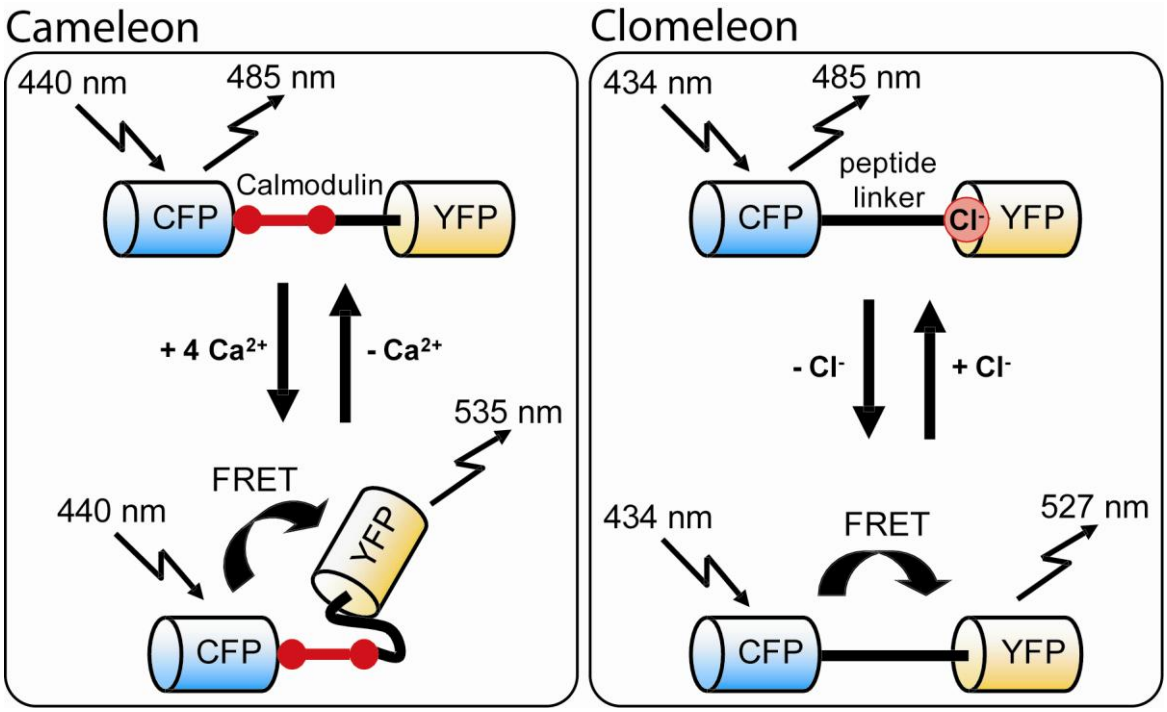

Figure 6. The functionality of the two ratiometric sensors.
Cameleon (left, modified after (MIYAWAKI et al., 1997)) and clomeleon (right, modified after (KUNER & AUGUSTINE, 2000)).

This results in a shift of the emitting fluorescence's wavelength from 485nm to 535nm and the calculated ratio increases. In addition to the spatiotemporal inhibitory pattern across the antennal lobe the cameleon measurements provided me with the corresponding excitatory pattern evoked by the same odors. Since these signals derive from the same neuronal subsets due to the GAL4:UAS system, they give me a combinatorial picture of the olfactory code in restricted areas of the olfactory system of *Drosophila melanogaster*.

2.4. Imaging

To acquire the imaging data all flies were imaged at a Till Photonics setup (Till Photonics GmbH), shown in Figure 7A, using a fluorescence microscope (Olympus, BX51WI) combined with a beam splitter (Optical Insights, DV-CC), to separate the two emitted wavelengths of 485nm and 535nm, and a CCD-camera (PCO Imaging, Sensicam). The whole setup was placed on a vibration cushioned table (Newport). The microscopes' object table was wired to a control unit for precise steering (Applied Scientific Instrumentation, Inc. MS 2000 XYZ Microscope Stage). A stimulus controller (Syntech, Stimulus Controller CS-55) produced the different air flows and a cold light source (Schott, KL 1500 LCD) illuminated the specimen for proper adjustments below the 20x water immersion objective (NA 0.95, XLUM Plan FI, Japan). The mentioned objective was used for the imaging of the antennal lobe but for the antennal imaging I utilized a 10x air objective (NA 0.30, UPlan FLN, Japan). The excitation light with the wavelength of 440nm was generated by a xenon lamp (Ushio UXL S150MO) in a monochromator (Polychrome V) from TILL Photonics and was guided onto the fly's brain via a glass fiber and a diochroitic mirror (Figure 7B). Emitted light passed the beam splitter and resulted in two movies with the different wavelengths of eCFP (485nm) and eYFP (535nm). The separated beams reached the chip of the CCD camera (charge coupled device) through a video/photo adapter (Olympus, UCMAD3). On the chip each of them was projected to one half of the 1376 x 1040 pixels. To increase the brightness it was possible to merge 4x4 pixels to one (Binning). The measurements were done with a frequency of 2Hz, i.e. two frames per second.

Using this setup I was capable of imaging signals on the antenna and within the antennal lobe evoked by odors. The odorants were prepared by pipetting 6µl on a small piece of filter

paper which was then placed inside a pasteur pipette (stimulus pipette). This stimulus pipette was connected to the stimulus controller, via a silicone tube, together with a second pipette without an odor (control pipette). Both were released into a continuous air flow, also originating from the stimulus controller and present for the whole measurement, which targeted the antenna of the dissected fly. The continuous air flow streamed with 1l/min onto the fixed fly and the added control flow with 0.5l/min. When the stimulus flow was switched on (also with 0.5l/min), the control flow was turned off. This was necessary since an increasing cumulative flow speed would have led to movement artifacts. A flowmeter (Cool Palmer ©, 0.4-5 LPM Air) controlled the stability of the adjusted flow speeds. The control experiments with potassium gluconate and γ-aminobutyric acid were accomplished by adding 20µl of a 1M solution of one of the components into the saline on the fly brain after all odors were tested. In contrast to this the two GABA blockers CGP and Picrotoxin were applied by exchanging the saline drop with 200µl of the respective concentration (5µM or 50µM).

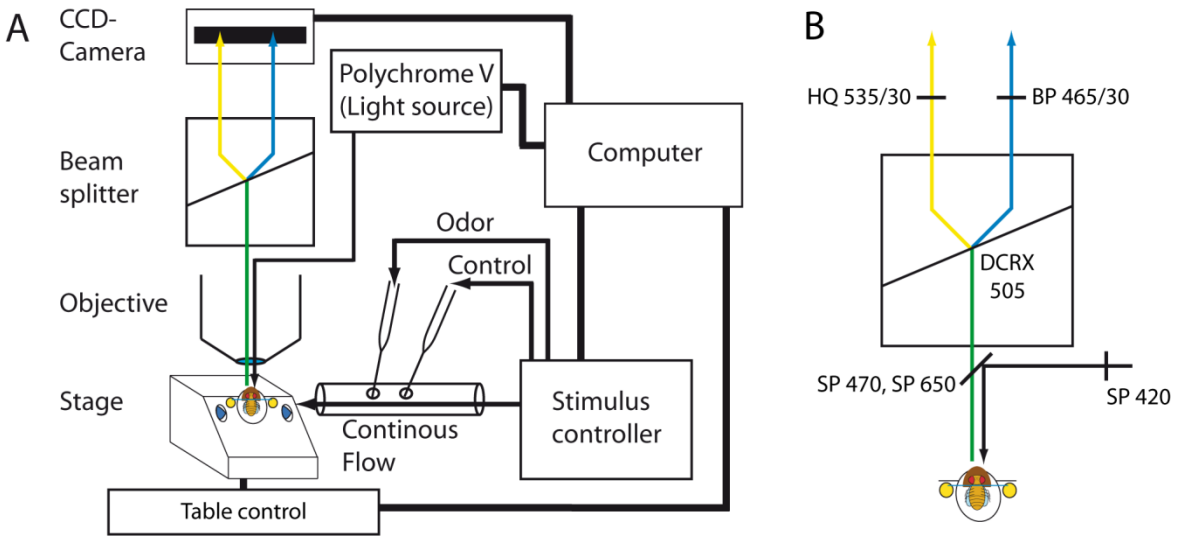

Figure 7. The imaging setup.
(A) The complete setup with the labeled light paths in direction of and from the fly brain as well as the continuous and stimulus air streams. **(B)** The magnified light paths of (A) with descriptions of the used mirrors, beam splitters and filters to separate the eYFP and eCFP wavelengths in different images.

2.5. Odorants and Stimulation

The mentioned stimulus controller was computer controlled and thus allowed to modify the characteristics of the odor puff. The major adjustable attributes were the starting point and the length of the stimulus. As a default setting the odor puff started 3s after the measurement was executed and lasted for 2s. A carbon filter inside the stimulus controller filtered the air before it was flowing through the tubes to prevent a contamination with surrounding odors. Additional to this precaution there was a row of small cavities behind the fly stage through which the air around was sucked off. Thus no odor remained at the flies surrounding to prevent a contamination of the following stimuli. By using a small but diverse set of odors I wanted to cover an adequate range of natural occurring scents which can be detected by the fly and posses a behavioral relevance in the fly's life. Table 2 shows the odor set. The corresponding chemical structures are shown in Figure 8. Since the most relevant scents for flies are emitted by rotting fruits most selected odors were esters which are the main components of these flavors but are also present in fresh fruits like *ethyl-3-hydroxy butyrate* (grape), *ethyl benzoate* (apple) and *isoamyl acetate* (banana). All 11 odors were diluted in mineral oil (BioChemika Ultra) which was also the control stimulus to check for bleaching.

Table 2. List of used odorants.
Except for *methyl hexanoate* odors were used at a concentration of 10^{-1}. *Methyl hexanoate* was applied at a concentration of 10^{-3} and 10^{-5}.

Odor	Abbreviation	Chemical class	CAS-Nr.	Source	Conc.
Anisole	ANI	Ether	100-66-3	SIGMA	10^{-1}
Benzaldehyde	BEA	Aromatic	100-52-7	SIGMA	10^{-1}
11-cis Vaccenyl acetate	CVA	Ester	-	Pherobank	10^{-1}
Ethyl-3-hydroxy butyrate	EHB	Ester	5405-41-4	SIGMA	10^{-1}
Ethyl benzoate	ETB	Ester	93-89-0	SIGMA	10^{-1}
Ethyl hexanoate	EHE	Ester	123-66-0	SIGMA	10^{-1}
γ-Valerolactone	GVL	Lactone	108-29-2	SIGMA	10^{-1}
1-hexanol	HEX	Alcohol	111-27-3	SIGMA	10^{-1}
Isoamyl acetate	ISO	Ester	123-92-2	SIGMA	10^{-1}
Methyl hexanoate	MHE	Ester	106-70-7	SIGMA	10^{-1}, 10^{-3}, 10^{-5}
Pentyl acetate	PEC	Ester	628-63-7	SIGMA	10^{-1}

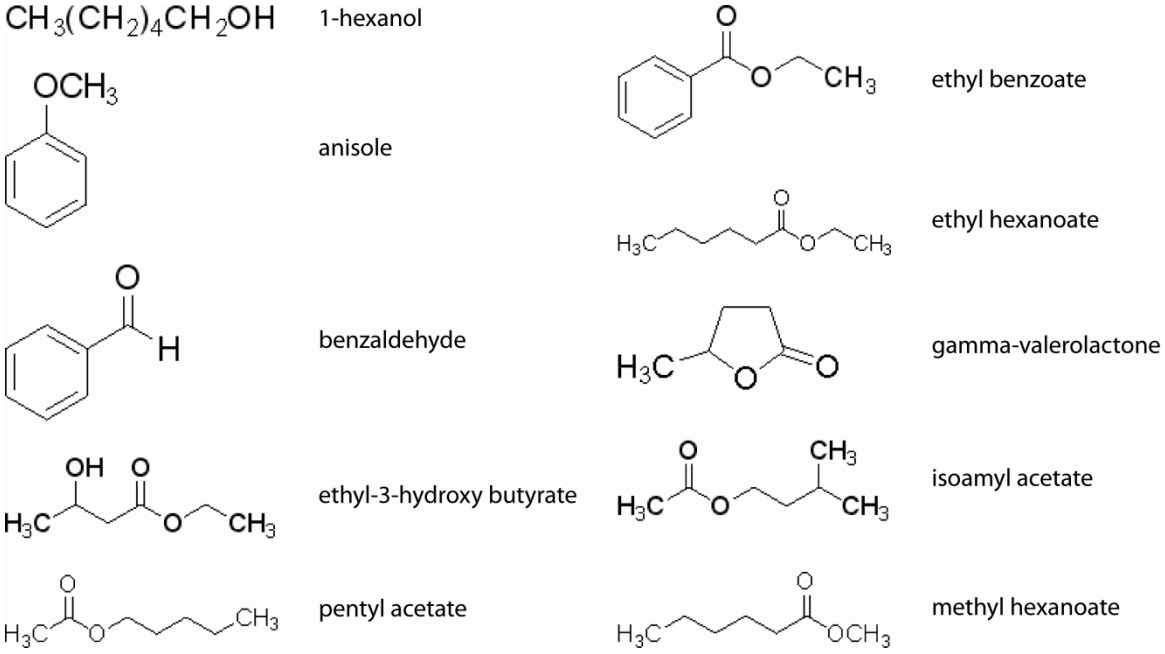

Figure 8. The chemical structures of the used odor set.

2.6. Data analysis

The obtained imaging datasets were first analyzed with TILLvisION (TiLL Photonics GmbH) and further data analysis was done with the program IDL (Version 6.4, Research Systems, USA). Each measurement consisted of the emission of eCFP on one side and the eYFP on the other side. With TILLvisION the movie was split into the two halves and the ratio of both was calculated (Figure 9) to obtain only the relative emission changes. Without this the effect the absolute brightness which differed between specimens would not have allowed to compare them. The handling of data was identical for clomeleon and cameleon. From this point on the data was further analyzed in IDL and at first the mentioned ratio was determined by dividing the eCFP images by the eYFP ones. From the resulting ratio a background correction was calculated by IDL. Therefore the average of the first 6 frames prior to the odor onset was subtracted from every single frame. This was necessary to adjust all traces so that they started at zero. Finally a manual movement correction was performed to compare the single frames per experiment and the experiments with each other to eliminate movement artifacts. To achieve the false color coded signals, the difference of the fluorescence before and during the odor application was calculated. Due to the dissimilar response kinetics of the two fluorophores, the time range for the signal calculation was different. For cameleon I

calculated the average fluorescent change between frame 8 (1s after stimulus onset) and frame 14 (2s after stimulus onset). The average emission changes for clomeleon with its slower response speed were calculated between the odors offset (frame 10) and 10s later (frame 30). In the resulting spatiotemporal patterns, coordinates were assigned to single glomeruli (coordinate size: 7x7 pixel equates 14x14 µm) to calculate individual time traces for identified glomeruli. To smooth the kinetics every three frames were averaged. The box plots of the continuative analysis calculated in SPSS were also based on the averaged ratios over animals and odors (e.g. Figure 15). The visualization and statistical analyses were accomplished with Excel (2007) and SPSS (17.0) as well as Adobe Illustrator (11.0). Statistical tests used were either the t-test or a Wilcoxon-matchpair test depending on the experiments.

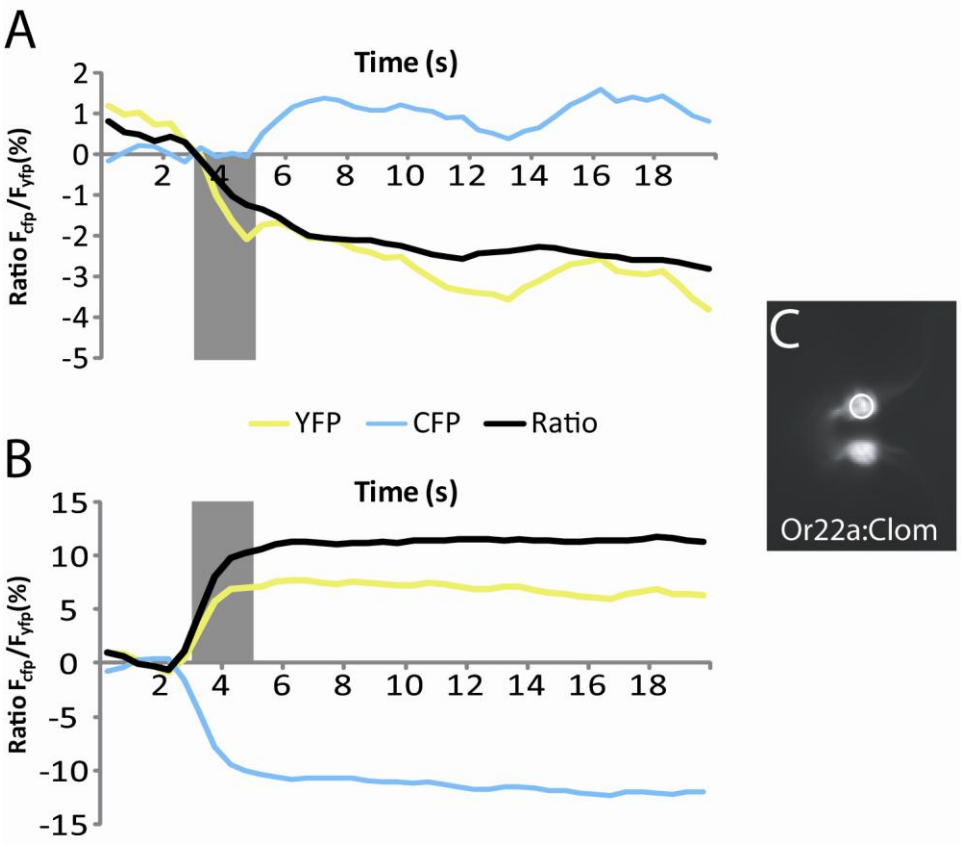

Figure 9. The separated kinetics of the two fluorophores YFP and CFP and their ratio evoked by *methyl hexanoate*.
(A) Kinetic of a single measurement of an OR22a;clomeleon fly and the separate kinetics of the fluorophores. **(B)** Kinetic of a single measurement of an OR22a;cameleon fly and the separate kinetics of the fluorophores. **(C)** Phenotype of the measured fly with the selected region for the measurement. The grey bar indicates the odor application for 2s.

2.7. Immunostaining

I carried out an immunostaining with the different transgenic fly lines to provide the basis for a reconstruction and identification of the imaged glomeruli. To do so, flies were first anesthetized with CO_2 and then fixed using 8% paraformaldehyde (0.2M) and Triton x-100 in phosphate buffer (PB) on a rocking shaker for 3h. Subsequent the fixative was replaced with a washing solution (0.2% Triton x-100 in Phosphate buffed saline (PBST)) to rinse the flies several times and over night at 4°C on a rocking shaker. The next step was to dissect the complete brains in the wash solution, to remove tracheas and to transfer them in a blocking solution (PBST with normal goat serum (NGS)). After 1h incubation at room temperature the blocking solution was replaced with the primary antibody solution (PBST-NGS, mouse α-nc82 (3%) and rabbit α-GFP (0.5%)) and incubated for two days at 4°C on a rocking shaker in darkness. The second antibody solution (PBST-NGS, α-mouse alexa 546 (0.5%) and α-rabbit alexa 488 (0.5%)) was added after another washing step with PBST and incubated for two days. Finally the brains were washed again with PBST and mounted with Vectashield (Vector Labs Inc.) on a glass slide. This immunostaining was performed with all three used GAL4 lines (OR22a, OR83b and GH146) to identify the glomerular structures. As a general background staining of the complete neuropil I used the mouse α-nc82 primary antibody in combination with the secondary antibody α-mouse alexa 546. This gave me an overview of the whole glomerular set without any affiliation of the single glomeruli to a tissue specific GAL4 driver (red staining in Figure 10A). To obtain this specificity I used the rabbit α-GFP primary antibody and combined this one with the secondary antibody α-rabbit alexa 488. Since clomeleon as well as cameleon consist of the two GFP derivates eCFP and eYFP, the GFP antibody could be used to label the two expressed fluorophores (green staining in Figure 10A). With the double staining I could see the specific neuronal subsets in a complete neuropil background and I was able to identify the single glomeruli. The complete immunostaining protocol can be found in the appendix. Figure 10A shows projections of confocal stacks generated from the stained brains. Unfortunately the resolution downgrades at deeper focal planes which made it difficult to identify the posterior and ventral glomeruli. To counteract this I used the 2-photon microscope (LSM 510 meta, ZEISS with 2-photon laser Chameleon, COHERENT) and produced *in vivo* stacks of the different GAL4 lines crossed with UAS-clomeleon since the 2-photon microscope produces crystal-clear scans also of the

deeper layers (Figure 10B). With the precise morphological overview provided by the immunostaining on one hand and the outstanding resolution in deeper tissue layers with the 2-photon microscope on the other, the identification of glomerular structures including the correlation of these glomeruli with spatiotemporal signals turned out to be much easier. In addition, the published OR specific spiking data from the HALLEM et al. publication(HALLEM & CARLSON, 2006) was used to confirm the glomerular identification of the odor induced calcium signals. With the experience gained from these identifications it was possible to assign the inhibitory signals to their glomerular origins as well.

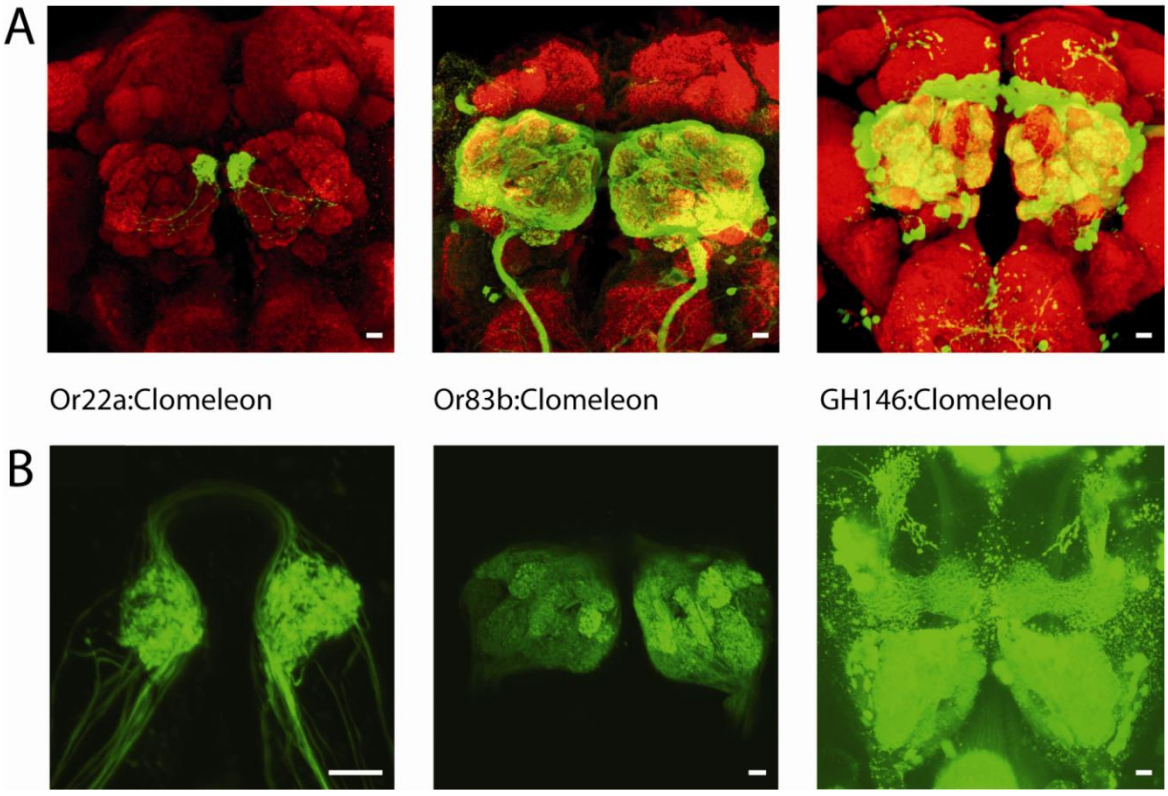

Figure 10. Projections of the fly brains.
(A) Projections made with the Zeiss LSM image browser on the basis of immunostained brain stacks produced with the confocal microscope. **(B)** Zeiss LSM image browser projections of *in vivo* stacks compiled with the 2-photon microscope. The scale bar indicates 10µm.

3. Results

The availability of clomeleon (KUNER & AUGUSTINE, 2000) in *Drosophila melanogaster* puts me in the position of visualizing odor evoked inhibitions in different olfactory neuronal populations with a focused point of view on chloride ions. This will be one important step towards a more complete understanding of the olfactory system in insects.

3.1. Verifying the function of clomeleon in the fly's olfactory system

To initially analyze the functionality of clomeleon throughout the olfactory system of *Drosophila melanogaster* I had to confirm that clomeleon actually reports changes in chloride ion concentration, which then would indicate an inhibition within the neuron. As an a priori control experiment I applied 20µl of 1M potassium gluconate (Figure 11C) directly into the saline upon the dissected fly brain to induce a strong excitation in the OSNs and PNs. Using the transgenic fly lines, OR83b and GH146, I was able to examine the effects in OSNs and PNs separately since these lines label the corresponding neurons via the GAL4:UAS system. Figure 11 shows a fast and steep decline of the clomeleon ratio immediately after the potassium gluconate was applied. This reports a strong increase of the intracellular chloride concentration possibly evoked by inhibitory postsynaptic potentials. Interestingly I observed the same response curve in OSNs (Figure 11B) as well as in PNs (Figure 11E). Both lack a clear recovery, except for the small rising towards the end in the OSN measurement. The percentage change of the clomeleon fluorescence in PNs was slightly stronger as in OSNs. This might indicate a higher number of GABAergic synaptic sites belonging to PNs that receive inhibitory lateral input from inhibitory LNs. The global effect of potassium gluconate on the antennal lobe is shown in Figure 11A and 11D where the raw morphological view (left side) is combined with the false color image of the same animal (right side) indicating the percentage fluorescence change of the clomeleon ratio. Red displays the strongest change and blue the weakest one. Every single false color coded image is scaled to its own min/max. To verify the role of the post- and presynaptic GABAergic sites in the mediation of chloride dependent inhibition is my upcoming goal.

Now that I know clomeleon is functional in the fly olfactory system it was necessary to verify that clomeleon is a reporter for inhibition. For that purpose I used γ-aminobutyric acid (GABA), an inhibitory neurotransmitter in the insect brain. Like above 20µl of a 1M solution of GABA (Figure 12C) were applied into the saline to induce a binding to the presynaptic GABA receptor sites of OSNs (OLSEN & WILSON, 2008) as well as to the postsynaptic ones of PNs (WILSON & LAURENT, 2005) artificially generating a lateral inhibitory input through the LNs. Therefore the signal pattern of the complete antennal lobe was taken into account to calculate the kinetics (Figure 12B and 12E) since the application treated all neurons identical. Figure 12 shows the resulting kinetics of the measurements for the OR83b- and GH146-GAL4 line. The first striking difference to the potassium gluconate curves was the time it took till a

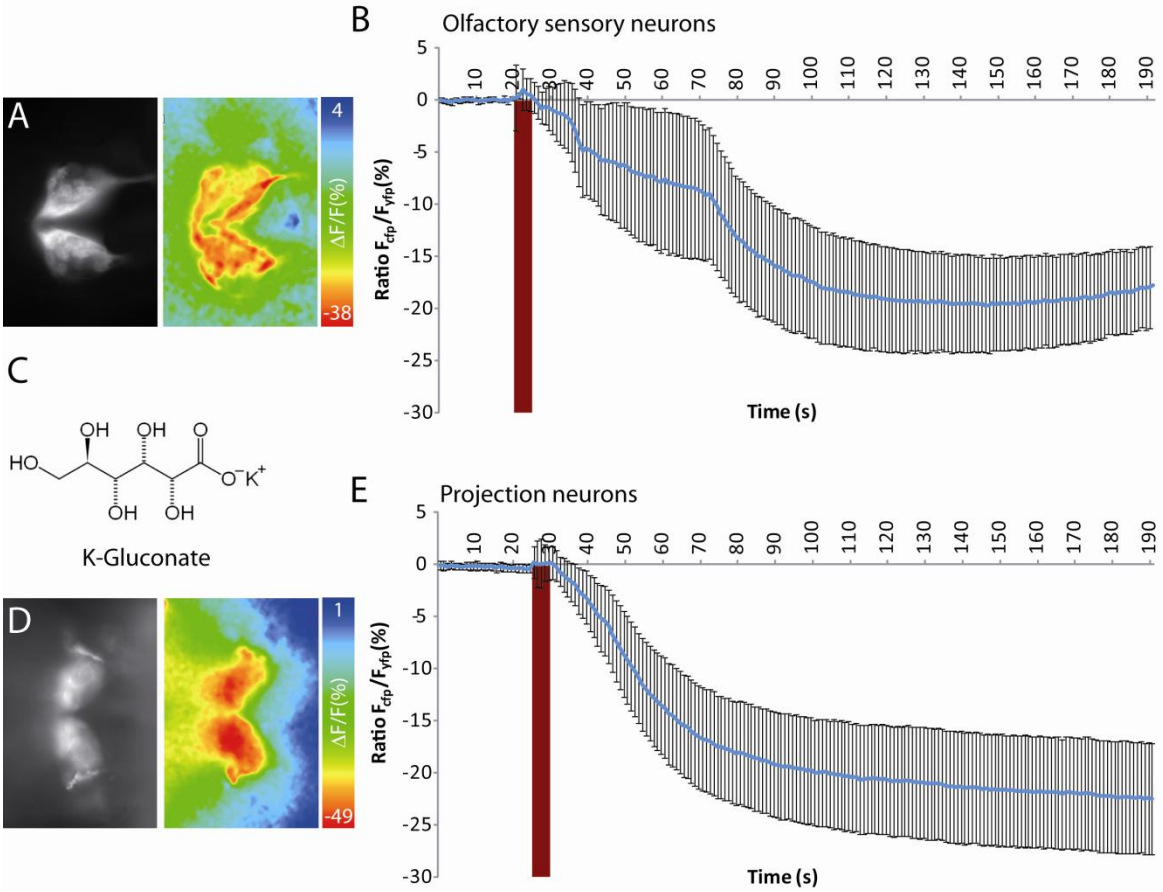

Figure 11. K-Gluconate effect on OSNs and PNs in the antennal lobe.
(A) Morphological view of the imaged OR83b-GAL4:UAS-clomeleon line (left) and the overlay of the false color coded signal pattern (right). **(B)** The application of K-Gluconate evoked a fast, strong and long lasting inhibitory signal in the OSNs (n = 5). **(C)** Chemical structure of K-Gluconate. **(D)** Morphological view (left) with the false color overlay (right) of the imaged GH146-GAL4:UAS-clomeleon line. **(E)** K-Gluconate also evoked a similar reaction in the PNs (n = 18). The red bar indicates the application of 20µl of 1M K-Gluconate into the saline. Data are represented as median ± STDEV.

strong reaction could be observed. At first both neuronal populations showed a slow and weak percentage decrease in fluorescence (phase 1). Then after 60s (OSNs) or up to 90s (PNs) a threshold was reached and the initially flat decrease was followed by a more steep one resembling the observations as seen with potassium gluconate but by far not as strong. The GABA induced percentage decrease was around 10 to 15%, whereas potassium gluconate decreased the fluorescence by 20 to 25%. The GABA effect showed a recovery phase after it reached its minimum. In Figure 12A and 12D the global effect of the applied GABA on all visible neurons is shown. In the GH146 image (Figure 12D) it was possible to see how the GABAergic inhibition was projected along the APTs. The observed recovery led me to the next experiment.

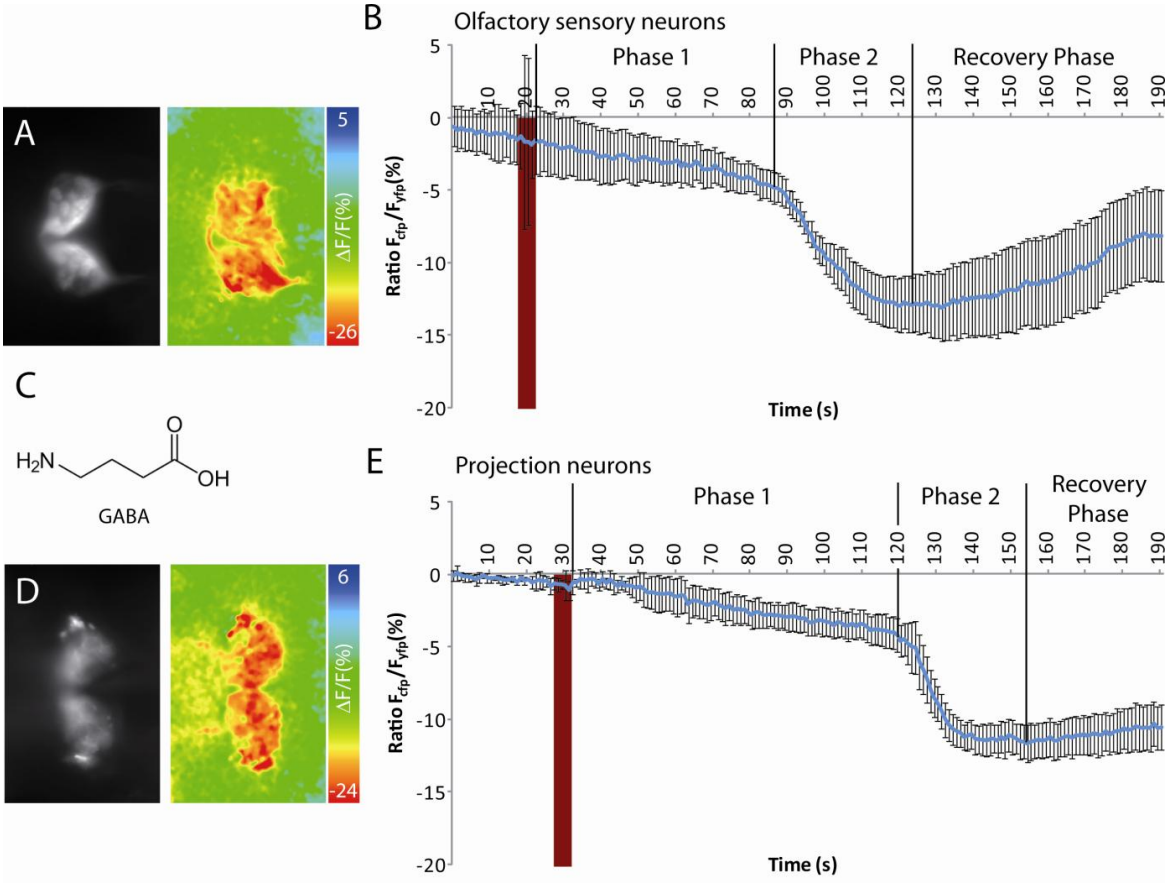

Figure 12. GABA effect on OSNs and PNs in the antennal lobe.
(A) Morphological view of the imaged OR83b-GAL4:UAS-clomeleon line (left) and the overlay of the false color coded signal pattern (right). **(B)** GABA evokes a biphasic response in OSNs (n = 9) **(C)** Chemical structure of GABA. **(D)** Morphological view (left) with the false color overlay (right) of the imaged GH146-GAL4:UAS-clomeleon line. **(E)** The PNs showed the identical response to GABA as the OSNs with a short delay (n = 6). The red bar indicates the application of 20µl of 1M GABA into the saline. Data are presented as median ± STDEV.

Since the clomeleon signals showed a rather slow kinetic contrary to the calcium ones measured with cameleon (see materials and methods), I wanted to know if these signals, which were extremely long-lasting in a neurophysiological way, monitored the actual intracellular chloride concentration or if they were an artifact of the fluorophores' own kinetic. For that purpose I measured the same odor, *ethyl-3-hydroxy butyrate*, several times in a row in the same OSNs with different interstimulus intervals (ISI). This experiment should show if the fluorophore, and with it the neuron, is excitable again before the measured ion concentration reaches the initial baseline and if the second treatment is somehow modulated by the first odor applications. Figure 13 shows the obtained results in a OR83b-clomeleon fly with two different interstimulus intervals, 60s and 120s, measured in the specific DM5 glomerulus, which gave one of the strongest signals evoked by *ethyl-3-hydroxy butyrate*. One can see that in Figure 13A the kinetic of the clomeleon was not able to return to baseline after 60s from the first *ethyl-3-hydroxy butyrate* application. The second odor puff resulted in an identical response regarding its amplitude. To complete the analysis I tested how long it actually took for the fluorescent signal to again reach the baseline. Therefore I tested an interstimulus interval of 120s. Figure 13B shows that the kinetic reached a plateau after around 100s from the first odor puff which was slightly lower than the baseline due to inevitable bleaching during the measurement. The repeated application of *ethyl-3-hydroxy butyrate* then again evoked a similar chloride signal as the initial odor puff. The glomerulus showed no sign of adaptation to the applied odorant within the given temporal specifications.

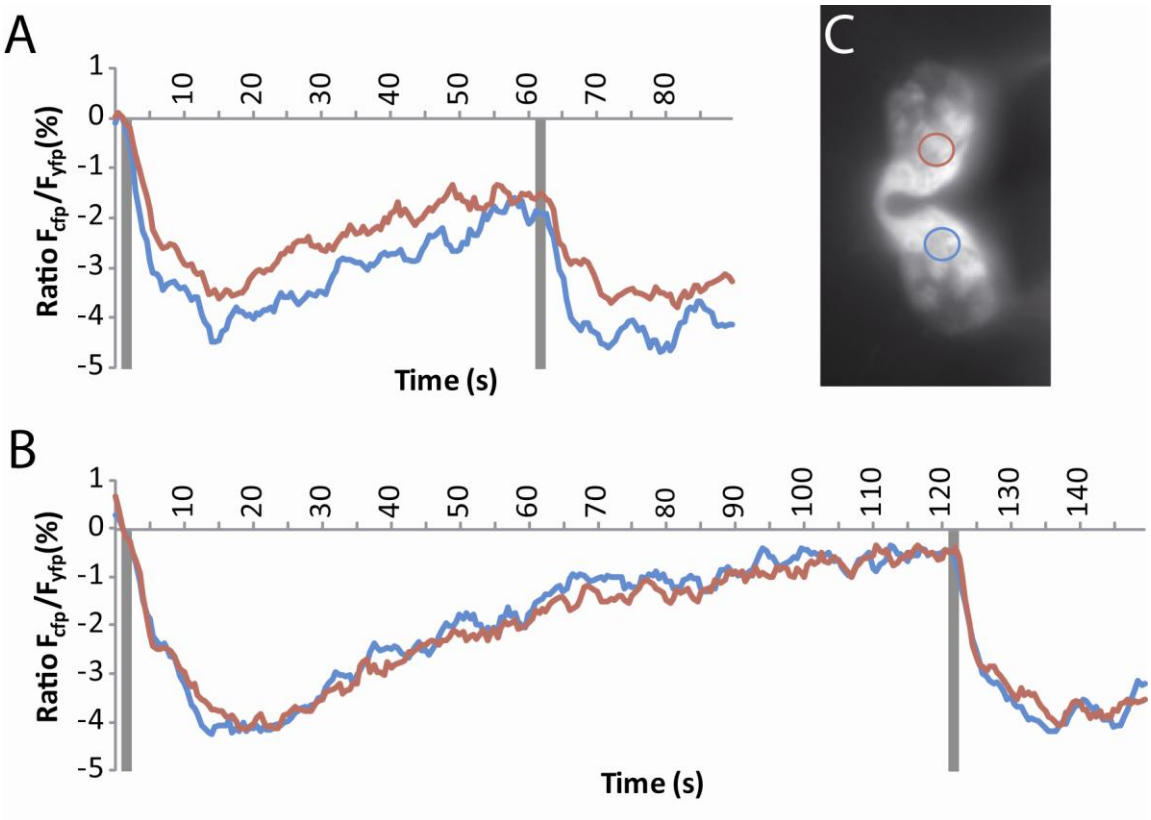

Figure 13. Repetitive stimulation of antennal lobe OSNs.
Different interstimulus intervals of 60s **(A)** and 120s **(B)** between the two consequential applications of e*thyl-3-hydroxy butyrate* (n = 1). The red line shows the kinetic of the left antennal lobe and the blue one shows the right one. **(C)** Morphological view of the imaged OR83b-GAL4:UAS-clomeleon line with an overlay showing the regions of interest (i.e. DM5 glomeruli) where the coordinates were placed. The grey bars indicate the odor application for 2 seconds. Data present the kinetics of a single specimen.

3.2. Odor induced clomeleon responses on the antenna

Before I started to analyze the functionalities of the chloride dependent inhibition within the antennal lobe of *Drosophila melanogaster* more precisely, I was curious if already the antenna was capable of giving me an insight in the peripheral neurophysiology of the targeted mechanisms. To obtain this insight I used the OR83b-GAL4 line to express clomeleon in the axons seen throughout the antennal lobe as well as in the corresponding dendrites of the OSNs. These are housed in the antennal sensillae, as well as the cell bodies. Luckily the fluorescence emitted by the OSNs in the funiculus itself and the sensillae was visible through the cuticular layer (Figure 14A) and could be imaged without any further dissection steps. Figure 14B shows the morphology of the antenna seen through the fluorescence microscope with a uniform expression pattern of clomeleon since nearly all OSNs express OR83b. Also one can see that in contrast to the morphological discrimination in Figure 14A the odor specific signals were not easily assigned to a distinct sensillar area but with the help of their own chloride time courses (as seen in Figure 14D) it was possible to distinct between them. The examples show that *ethyl-3-hydroxy butyrate* gave the strongest chloride signal of the three odors in every area and was always evoking a negative plateau without recovery during the measurement. In contrast to that the application of *benzaldehyde* resulted in a broad negative peak with a recovery almost to the initial baseline. Furthermore *1-hexanol* induced a weak negative clomeleon response without recovery. Due to the weakness of the chloride signals it was difficult to distinguish them from sole movement by just looking at the signals. However, as shown in Figure 14B it was easier to distinguish them when observing the spatial distribution over the whole antenna. Figure 14 also shows that the clomeleon signals were intraspecific conserved.

In addition to the descriptive attributes of the specific odor kinetics it was possible to distinguish them by the distribution of inhibited dendrites over the whole antenna. Since single ORs are expressed in a small subset of neurons which is restricted to a special type of sensilla and therefore also to a morphological area (VOSSHALL et al., 1999; FISHILEVICH & VOSSHALL, 2005) it is possible that odorants can be discriminated by their unique antennal pattern. To examine this I tested the odors used in Figure 14 and screened the anterior side of the funiculus for the mentioned patterns. One can see that the clomeleon signals in

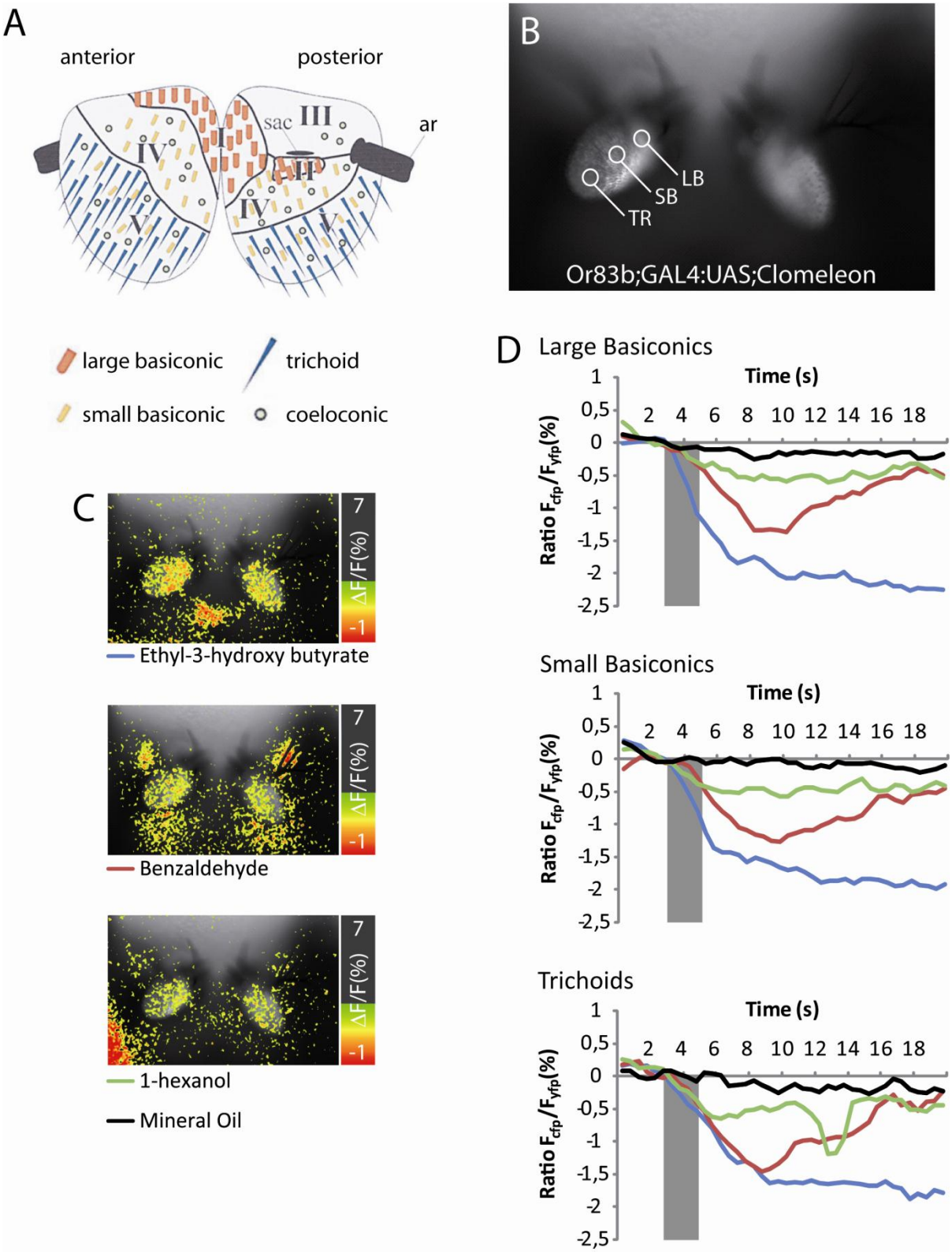

Figure 14. Odor induced chloride signals on the antenna.
(A) Distribution of the different sensillar types across the anterior and posterior side of the antenna (ar = arista, sac = sacculus; de BRUYNE et al. 2001). **(B)** Morphological view of the antenna of an OR83b-GAL4:UAS-clomeleon fly with the marked regions of interest where the coordinates were placed. **(C)** Overlay of the false color coded chloride signals of *ethyl-3-hydroxy butyrate*, *benzaldehyde* and *1-hexanol* on the morphological view in A. **(D)** Clomeleon signals of the three odors separated by the sensilla area according to the coordinates in A (n = 7). The grey bar indicates the odor application for 2s. Data are represented as median values.

Figure 15B and 15C show a uniform distribution throughout the three different antennal zones making it impossible to discriminate them from each other just by judging the signal strength between the regions. However, what is also apparent is the overall signal strength on the antenna which was differing for several odors. *Ethyl-3-hydroxy butyrate* was giving the strongest chloride signal across the anterior side of the funiculus in every sensillar area and *benzaldehyde* was giving the second strongest one in all regions. The other odorants grouped below these two also without distinct varieties regarding the different sensillar areas.

To describe the discriminative ability of chloride concentration changes compared to calcium I tested the same odors in the same setup using OR83b-GAL4:UAS-cameleon flies to image the identical neuronal set. Figure 15A shows the calcium signals from the antenna. As one can see, the calcium signals were as broadly distributed as the ones observed with clomeleon without any striking differences between the sensillar regions. However, the trichoid sensillar area which showed a significantly lower signal as the two basiconic ones for *ethyl-3-hydroxy butyrate* and a higher response for *11-cis vaccenyl acetate*, the only known sexual pheromone in *Drosophila melanogaster* (WANG & ANDERSON, 2010; BRIEGER & BUTTERWORTH, 1970; BUTTERWORTH, 1969). Compared to the clomeleon signals an obvious similarity was that *ethyl-3-hydroxy butyrate* gave a strong excitatory as well as an inhibitory signal in the same region except for the trichoid sensilla. The other odors tested evoked intermediate responses in both cases, calcium and chloride increases. The application of *benzaldehyde* led to a stronger inhibitory signal and *pentyl acetate* evoked a heavy excitatory response almost as big as the one observed for *ethyl-3-hydroxy butyrate* in contrast to an almost not existent inhibitory reaction.

I have to admit that the possibilities to discriminate odors on the antenna with the help of the clomeleon signals are very restricted in the global OR83b lines since the imaged signals are mainly uniformly spread in the three selected sensillar regions. The usage of more special OR lines could possibly provide me with the necessary precision to distinguish different odor induced chloride responses already on the antenna. However, I will first present the odor evoked signals within the antennal lobe to analyze whether the chloride signals are globally spread or if I can observe a glomerulus-specific, spatiotemporal pattern as seen with calcium-sensitive proteins (PELZ et al., 2006; FIALA & SPALL, 2003).

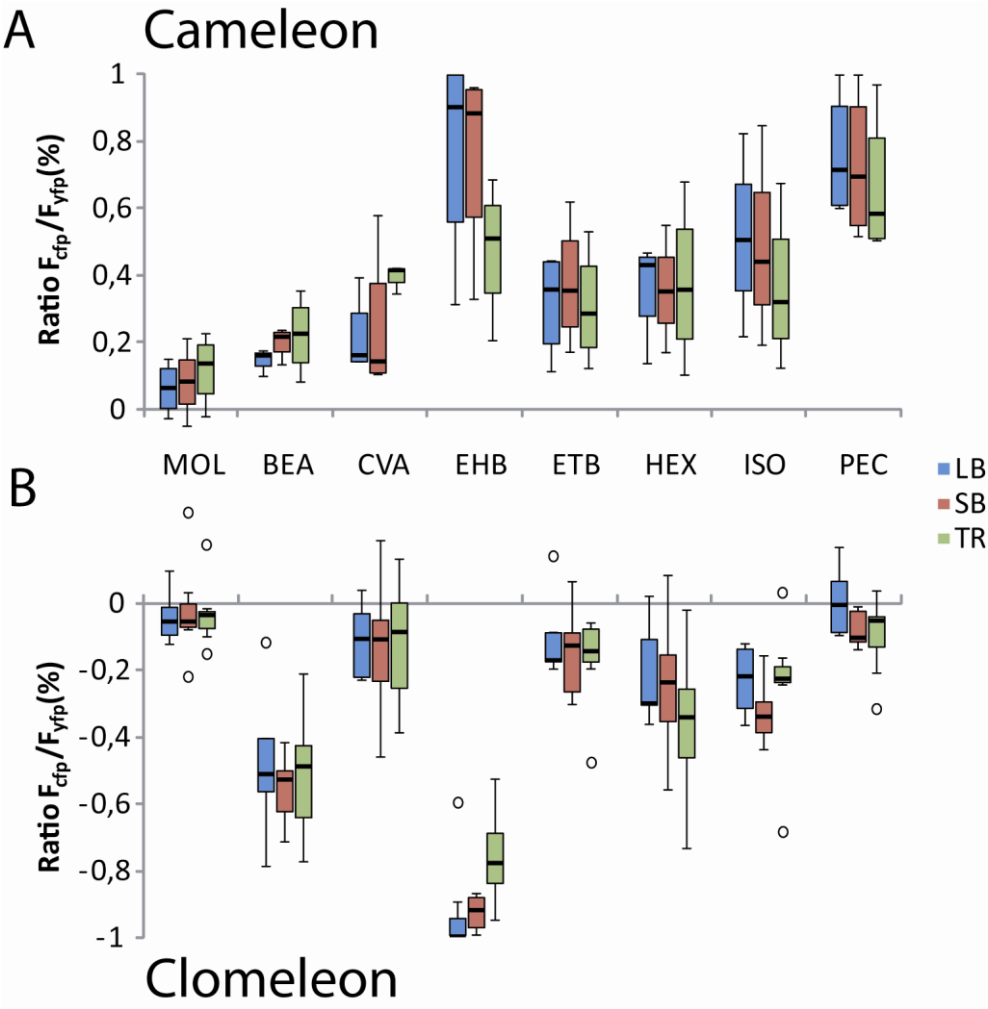

Figure 15. Chloride and calcium signals on the antenna.
(A) Cameleon signals in the three sensillar areas (*n* = 4). **(B)** Clomeleon signals in the corresponding regions (*n* = 7). LB = large basiconic, SB = small basiconic, TR = trichoid. The box plots represent the median value (horizontal line inside the box), the interquartile range (height of the box, 50% of the data are within this range) and the minimum and maximum value (whiskers) of each experimental group. Circles depict outliers with values that were more than 1.5 times the interquartile range from the lower or upper quartile.

3.3. Clomeleon in the antennal lobe

Continuing the analysis of the inhibitory contribution to reception, transduction and projection permitted by single component odorants throughout the first level of the olfactory system in *Drosophila melanogaster*, I imaged a set of odors in the antennal lobe. Therefore I used the OR83b-GAL4:UAS-clomeleon line to image inhibitory odor responses in almost all OSNs at a time (VOSSHALL et al., 2000). Figure 16 shows the representations of the odorants by single traces detected on the sensory level of a selected set of four glomeruli. The glomeruli are DL5 (OR7a), lying dorsolateral, DM3 (OR33b/OR47a) and DM5 (ORr33b/OR85a), placed more medial, and VA6 (OR82a), a ventral lying glomerulus in the anterior region (STOCKER et al., 1990). All four glomeruli were easy to identify by position or with the help of their odor specific responses. A clear distribution of signals was recognizable since most of the odors evoked chloride signals in a specific set of glomeruli. Additional information gave the signals' amplitude as well as the temporal characteristics indicating unique response dynamics of single olfactory receptors when interacting with different odorants. Figure 16 shows the chloride signals evoked by a set of four odors including *ethyl-3-hydroxy butyrate*, which already showed a strong response on the antenna, and furthermore *1-hexanol*, *benzaldehyde* and *pentyl acetate*. In Figure 16B the odor induced chloride signals are shown. *Ethyl-3-hydroxy butyrate* evoked a strong response in a large set of dorsomedial glomeruli. This broad pattern made it difficult to distinguish all glomeruli only with one odor signal but in our subset of four glomeruli it was clear that the DM5 glomerulus gave the strongest response. The other odors generated more restricted clomeleon responses in the antennal lobe. The strongest response was induced by *1-hexanol* and inhibited glomeruli situated medial and anterior to the DM5 glomerulus. *Benzaldehyde* showed an even more restricted pattern consisting only of the DL5 glomerulus as well as of glomerulus VM3 which was already inhibited by *1-hexanol*. A broader spatiotemporal inhibitory pattern was induced by *pentyl acetate* which covered a similar area as *ethyl-3-hydroxy butyrate* but gave a stronger response in the DM3 glomerulus. The VA6 glomerulus showed a similar weak inhibition to all four odors tested.

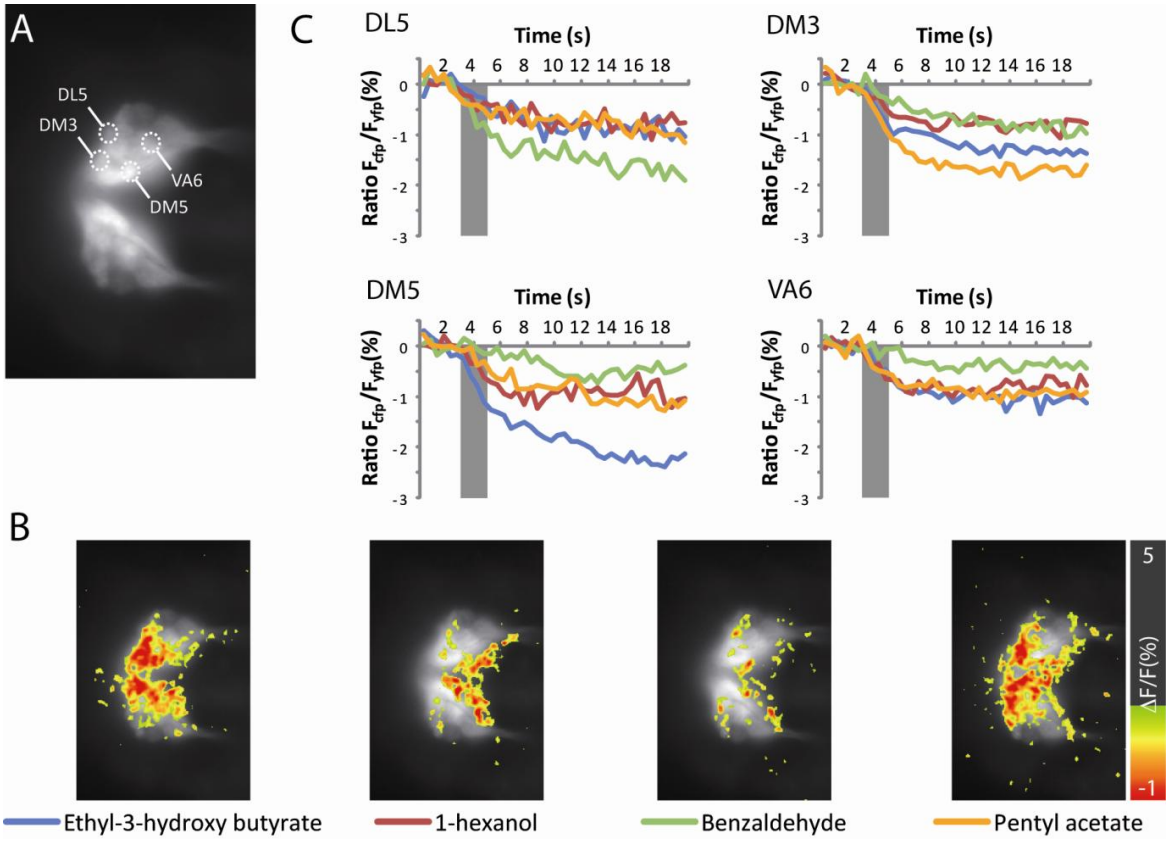

Figure 16. Single odor traces measured with clomeleon in OSNs in the antennal lobe.
(A) Morphological view of the OR83b-GAL4:UAS-clomeleon fly with the four selected glomeruli (DL5, DM3, DM5 and VA6). **(B)** False color coded overlay of the chloride signals of *ethyl-3-hydroxy butyrate*, *1-hexanol*, *benzaldehyde* and *pentyl acetate* onto the morphological view in A. **(C)** Single time traces of the four odors imaged in the selected glomeruli. The grey bar indicates the odor application for 2s. Data are represented as MEAN (n = 9).

Next, I analyzed how the gathered information from the primary sensory level is displayed in the PNs after the antennal lobe's processing took place. Therefore I used the GH146-GAL4:UAS-clomeleon line, which allowed imaging a large set of PNs from the anterodorsal and lateral cell clusters (STOCKER et al., 1997) at a time. As already seen for the OSN level, single odorants were capable of evoking chloride signals only in specific glomeruli. This chloride signals varied in amplitude and slope characteristics within a single glomerulus which made it possible to identify an odor simply by judging the spatiotemporal pattern of its chloride responses.

3.4. Applying a functional clomeleon map

In order to map the odor signals to identified functional units, i.e. the olfactory glomeruli, it is necessary to have a glomerular map or an atlas. The literature provides us with a couple of precise atlases (LAISSUE et al., 1999; COUTO et al., 2005; STOCKER et al., 1990). The problem with these atlases is that they are created on the basis of completely extracted brains of *Drosophila* and therefore do not reflect the exact orientation inside the head capsule. One main issue is that extracted brains lack the tension caused to the antennal lobe by the attached antennal nerve and therefore especially the dorsal most glomeruli are not situated in their natural position. To counteract this I used another approach. Instead of dissecting the brains out of the head to do immunostaining I used the OR83b and GH146-GAL4 lines to express clomeleon or cameleon in the target tissues and scanned *in vivo* stacks with a 2-photon microscope (Figure 17A). On the basis of these stacks I reconstructed and identified the labeled glomeruli. First of all this technique has the advantage that only glomeruli which were seen in the imaging were incorporated in the reconstruction. Secondly, the antennal nerve was still attached and with it the caused tension. Third, the point of view on the antennal lobe was exactly the same in the reconstruction and the physiological measurements. Figure 17A shows a series of sections of one *in vivo* stack made with the 2-photon microscope. Based on this stack the reconstruction in Figure 17B was generated in AMIRA (Version 5.2.1). Unfortunately I could not identify every single glomerulus with the help of the available atlases since even they often showed a lack of accuracy in the identification. I did this for the glomeruli labeled by the OR83b-GAL4:UAS-clomeleon and GH146-GAL4:UAS-clomeleon line to compare the set of OSN and PNs, respectively. It turned out that OR83b (Figure 17C right) included every known dorsal lying glomerulus visible in the conventional imaging. A problem in this reconstruction generated from a single specimen was the esophagus since it pushed the ventromedial glomeruli (VM2 and VM3) as well as the DM2 glomerulus slightly underneath the dorsomedial ones. Because of this it was necessary to think of these three as more prominent glomeruli beside the DM5 and DM6 glomerulus. Having completed the reconstruction of the GH146 fly line I observed a single difference in the dorsal glomerular pattern as the VM5 glomerulus lacked innervations of PNs belonging to the GH146 line (Figure 17C left). Further differences regarding the innervation patterns of the two GAL4 lines were obvious in the ventral layers (Figure 17B and 17E).

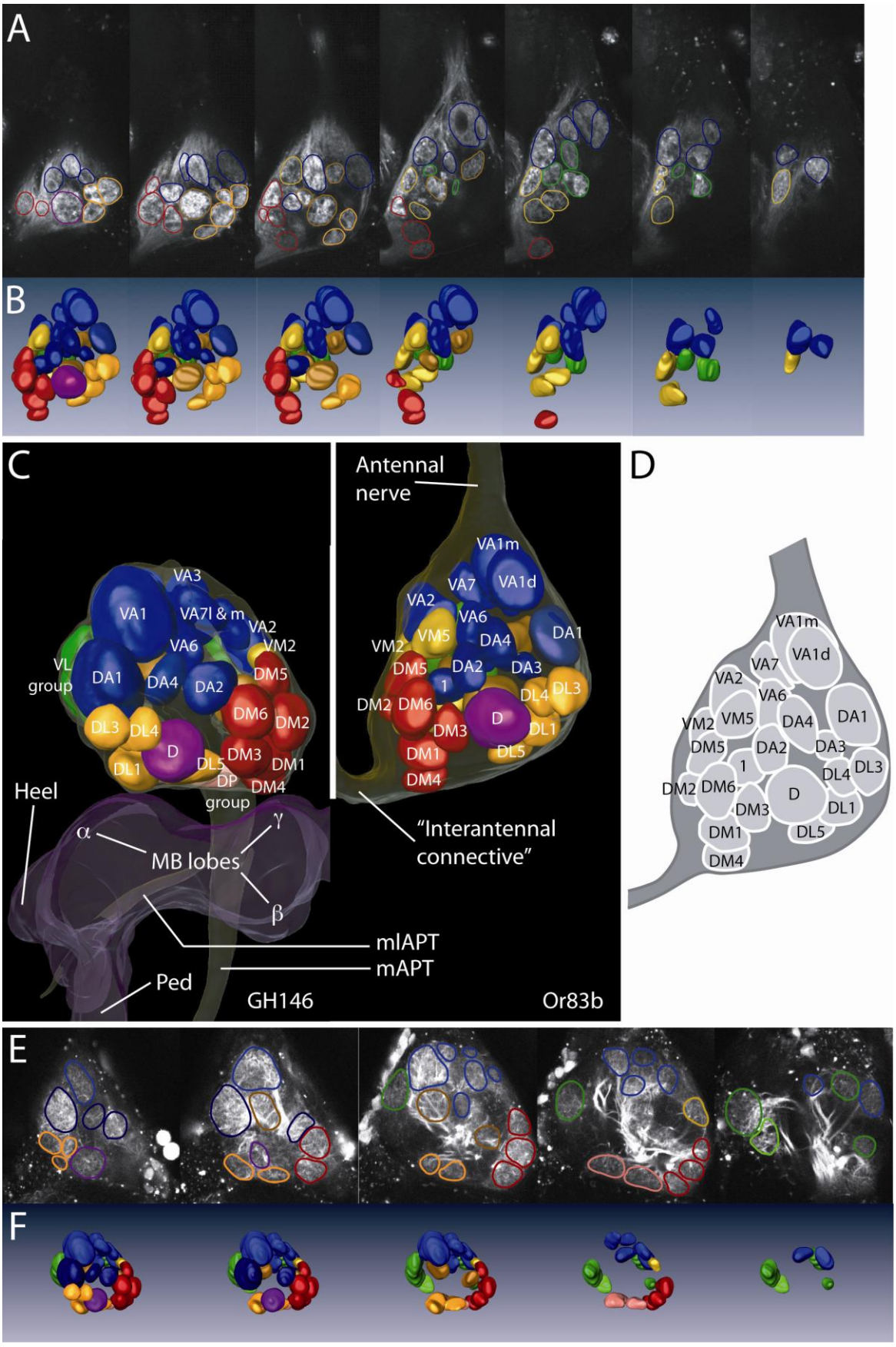
A
B
C
Antennal nerve
VA3
VA1
VA7l & m
VA2
VA6
VM2
VL group
DA1
DA4
DA2
DM5
DM6
DM2
DL3
DL4
D
DL1
DM3
DL5
DM1
DP group
DM4
Heel
α
γ
MB lobes
β
mlAPT
mAPT
Ped
GH146
VA1m
VA7
VA1d
VA2
VA6
VM2
VM5
DA4
DA1
DM5
DA2
DA3
1
DL4
DL3
DM2
DM6
D
DL1
DM3
DL5
DM1
DM4
"Interantennal connective"
Or83b
D
VA1m
VA1d
VA7
VA2
VA6
VM2
VM5
DA4
DA1
DM5
DA2
DA3
1
DL4
DL3
DM2
DM6
D
DL1
DM3
DL5
DM1
DM4
E
F

In the ventral area it was difficult to identify all glomeruli but clearly the sets were not congruent with each other. For example the GH146 line included almost the complete ventrolateral glomerular set which was totally absent in the OR83b line. In addition the ventroanterior and the ventromedial region of the antennal lobe incorporated more labeled glomeruli in the GH146 line. Due to the fact that these glomeruli were mostly concealed by the dorsal ones they could not be measured in the conventional imaging experiments.

3.5. Comparing the processing levels within the antennal lobe

What is even more interesting than the informing characteristics of the single neuronal levels is the comparison of the different processing levels, i.e. the sensory input versus the projecting neuron output, possibly giving insight into the processing mechanisms taking place within the antennal lobe. The results recorded from PNs and OSNs for the same set of odors (partly shown in Figure 16) might indicate more than one way of processing mechanism. In order to compare the signals imaged in the PNs with the ones from the OSNs in a more figurative way (Figure 18), I used color coded categories to describe the percentage change of response intensity in a schematic glomerular map. *Ethyl-3-hydroxy butyrate* evoked the strongest signal of the odors tested in the OSNs, as seen on the antenna (Figure 15B), and evoked a specific spatiotemporal pattern across the glomeruli in the antennal lobe. Other odors like *pentyl acetate* evoked almost no chloride signal on the antenna but induced a strong response in single glomeruli. For *benzaldehyde* it was the other way around, i.e. I could observe the second largest signal on the antenna but only sparse responses in the antennal lobe.

Figure 17. Reconstruction of an *in vivo*OR83b;clomeleon and GH146;clomeleon brain.
(A) Sections of an OR83b-GAL4:UAS-clomeleon stack of the right antennal lobe from dorsal to ventral. **(B)** The reconstructed glomerular pattern in 3D in the corresponding levels to A. The color code indicates the morphological position of the glomeruli (purple = dorsal (D), red = dorsal medial (DM), orange = dorsal lateral (DL), dark blue = dorsal anterior (DA), yellow = ventral medial (VM), light blue = ventral anterior (VA), brown = dorsal central (DC), green = ventral central (VC)) **(C)** The complete reconstructions in combination with the antennal lobe and mushroom body structure (DP = dorsal posterior, mAPT = medial antennoprotocerebral tract, MB = mushroom body, mlAPT = mediolateral antennoprotocerebral tract, Ped = pedunculus, VL = ventral lateral). **(D)** A simplified map with the identified glomeruli. **(E)** Sections of the confocal stack with corresponding levels to F.**(F)** The 3D-reconstructed glomerular pattern of the GH146-GAL4:UAS-clomeleon line scanned in the same levels as in E (extended color code: pink = dorsal posterior (DP), dark green = ventral lateral (VL) & ventral medial (VM)).

Continuing the analysis I concentrated on the chloride signal transmission from the OSNs to the PNs. Since the PNs form the actual gateway to higher brain centers the information that their axons forward should undergo already primary processing within the antennal lobe. By comparing the chloride patterns between OSNs and PNs for the same odors it is obvious that in almost every case the patterns show strong differences between the two levels (Figure 18B and 18C).

In the case of *benzaldehyde*, *isoamylacetate* and *11-cis vaccenyl* acetate the OSNs showed a sparse chloride signal pattern restricted to a few glomeruli. In the PNs the odors evoked a broad and strong inhibitory pattern which was stronger for *benzaldehyde* than for *isoamylacetate* and *11-cis vaccenyl acetate*.

Considering the chloride responses to *pentyl acetate* another observation can be made: a wide inhibitory glomerular pattern at the OSN level is shifted to an output pattern that includes even more glomeruli. In addition a few glomeruli are inhibited at the OSN, but not at the PN level.

E*thyl-3-hydroxy butyrate* and *1-hexanol* showed a distinct pattern of glomeruli that are strongly and some just slightly inhibited at the OSN level. Both odors induced a similar inhibitory pattern at the PN level but the patterns itself changed quite strongly. The signal intensity is much less in single glomeruli (VA2 and DM1) and other glomeruli gained stronger chloride signal intensity (DM5 and several DLs). This effect shows a “shift” of the chloride

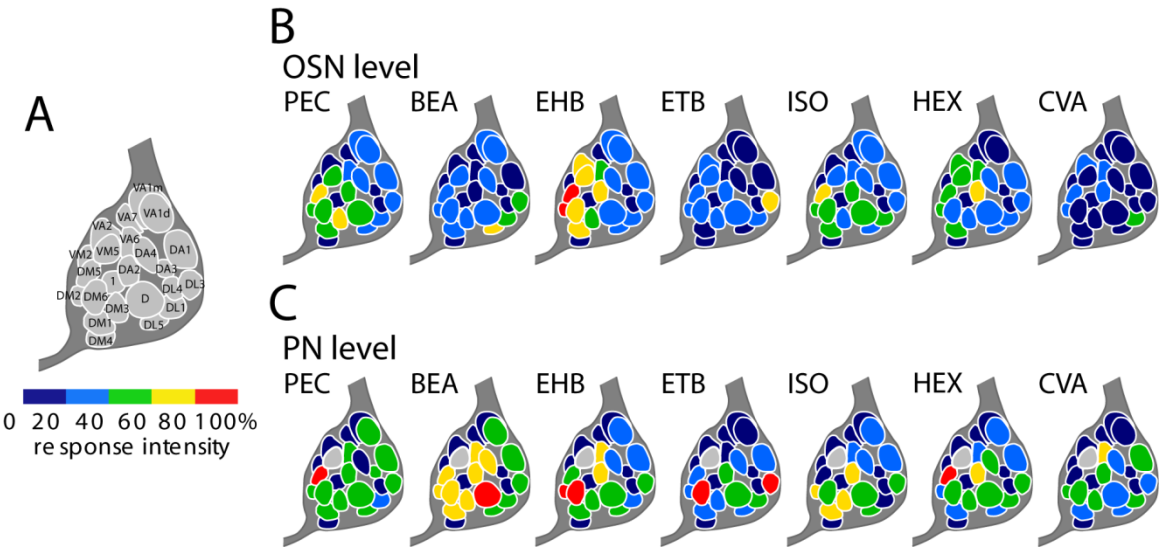

Figure 18. Chloride signals in the antennal lobe in OSNs and PNs.
(A) Glomerular map based on the 3D-reconstruction. **(B)** Odor specific signal pattern in OR83b-GAL4:UAS-clomeleon flies. **(C)** Odor specific signal pattern in GH146-GAL4:UAS-clomeleon flies.

signal from the anteromedial region to the dorsolateral and dorsomedial glomerular areas in both cases.

A further observed mechanism is the signal shift of *ethyl benzoate* whose strong inhibitory response in OSNs was restricted only to the DL3 glomerulus. At the output level this signal became even stronger and one additional glomerulus (DM6) which displayed only a weak response previously now was strongly inhibited too.

The signal shifts between OSNs and PNs are depicted in Figure 19 and represent the observed differences between input and output chloride responses. The inhibitory responses induced by *benzaldehyde*, *isoamylacetate* and *11-cis vaccenyl* acetate increased in glomeruli at the PN level where there was little or even no chloride response visible at the input level. Furthermore *pentyl acetate* represents a distribution of the chloride signal by a slight increase and decrease in a wide set of glomeruli. Also the "shift" in the pattern described for *ethyl-3-hydroxy butyrate* and *1-hexanol* is apparent since they both showed a signal decrease in three to four glomeruli and an increase in even more ones. Finally, the modulation of *ethyl benzoate* is most prominent in the DM6 glomerulus plus a slight amplification in the surrounding glomeruli. These weak signal increases in the surrounding glomeruli also push the DL3 to the same level as the DM6.

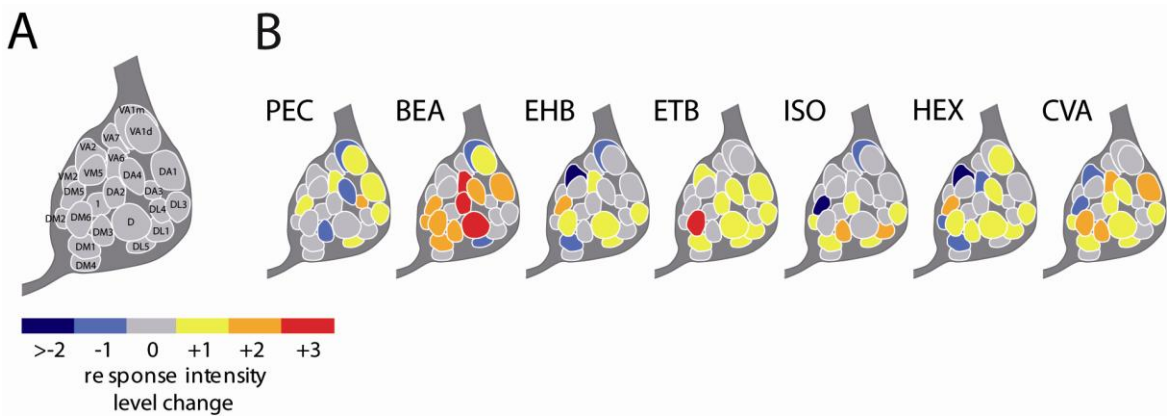

Figure 19. Calculated differences between the chloride responses on the input and output level. **(A)** Glomerular map based on the 3D-reconstruction. **(B)** Response intensity level change based on a comparison of the OSN and PN clomeleon signals shown in Figure 18.

3.6. Contribution of GABA to the inhibitory signals

In the beginning I was able to prove that GABA affects the clomeleon reported and chloride mediated inhibitory pathway in the antennal lobe by applying it directly into the saline on the dissected brain. The known role of GABA as an inhibitory neurotransmitter in the central nervous system of *Drosophila melanogaster* supported the potential function of clomeleon as a chloride sensor. Although GABA itself has a clear defined chemical structure its functionalities in the insect brain are eclectic because of the versatile distribution of the two different receptors known in the fruit fly. These two receptors are the $GABA_A$–type and $GABA_B$–type receptor which mediate two diverse pathways of signaling along the synapses where they are located. The $GABA_A$-type receptor is an ionotropic receptor permitting a fast, directly chloride dependent, inhibitory signal and the $GABA_B$-type receptor is a slower metabotropic receptor which acts per G-protein coupling (KAUPMANN et al., 1997). To dissect the contribution of each of the two receptors regarding the measured inhibitory odor signals, I tested the odor *ethyl-3-hydroxy butyrate* during the application of different GABA receptor blockers. First I used the blocker picrotoxin (PTX) which is known to be an efficient competitive $GABA_A$ antagonist. To block $GABA_B$-type receptors I used the antagonist P-(3-aminopropyl)-P-diethoxymethylphosphinic acid (CGP54626) which has been shown to be effective in *Drosophila* (WILSON & LAURENT, 2005). I tested them in the usual imaging setup by replacing the saline with a blocker-saline solution of different concentrations and tested the odor response every time after a new concentration was applied onto the brain. I used the GH146-GAL4:UAS-clomeleon line since most of the described lateral GABAergic input that arises from the LNs is postsynaptic affecting mainly the PNs.

Figure 20 shows the effect of the antagonists in a single specimen (left) and the summarized results over the whole experiment (right, n = 9). In the examples one can clearly see that both blockers were capable of decreasing the inhibitory chloride signal evoked by *ethyl-3-hydroxy butyrate*. The application of 5µM CGP54626 actually was able to completely abolish the signal, while PTX only lowered the signal amplitude (Figure 20C). Interestingly the PTX traces also showed a concentration dependent effect as 50µM decreased the signal slightly more than 5µM. However, the signal was still not completely eliminated (Figure 20A). Another difference between the two blockers was the wash-out phase where the blocker solution was exchanged with pure saline. PTX could only be washed out partly. The signal

recovered to a reduced level compared to before. In the case of CGP54626 the recovery in the example is more obvious as it is returning to the same level as before the treatment with the antagonist.

In summary, the effect and recovery of the *ethyl-3-hydroxy butyrate* chloride signal under the influence of CGP54626 is clearly visible since the measurements prior and after the treatment were significantly different from the measurements during the CGP54626 treatment (Figure 20D). Regarding PTX a similar clear effect is visible although only the signal decreasing effect of the 5µM concentration was significantly different compared to the saline measurement. The higher PTX concentration of 50µM showed no stronger decrease then the initial one. Furthermore the wash-out of PTX did not result in a significant recovery of the effect suggesting a less reversible binding to the receptor (Figure 20B).

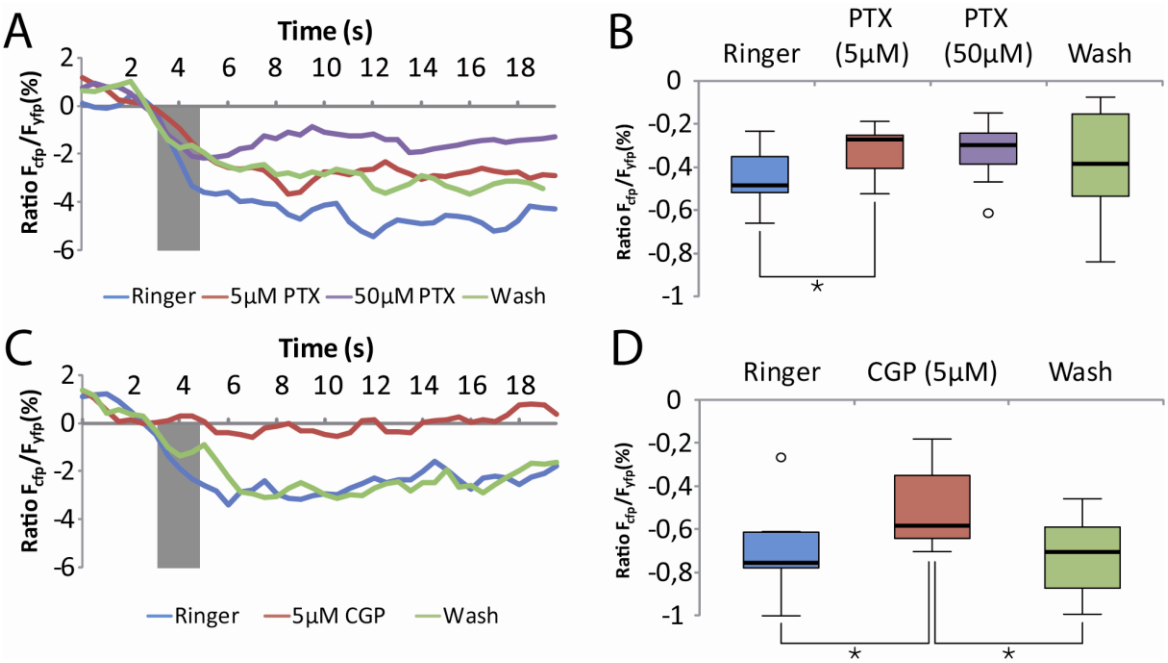

Figure 20. Modulatory effects of PTX and CGP54626 on antennal lobe PNs.
(A) Single time trace of a GH146-GAL4:UAS-clomeleon fly. The application of different PTX concentrations (5 and 50µM) alters the inhibitory signal strength of *ethyl-3-hydroxy butyrate* without complete recovery after wash-out. **(B)** Averaged results for the two PTX concentrations (n = 9). **(C)** Single time trace of a GH146-GAL4:UAS-clomeleon fly. CGP54626 in a low concentration of 5µM abolishes the complete inhibitory signal. **(D)** Averaged results for the CGP54626 measurements (n = 9) (*p<0.05). (A, C) Data present the kinetics of a single specimen.

3.7. Clomeleon and cameleon signals in an OSN subset on the antenna and within the antennal lobe

After having studied the general functionalities of clomeleon in the olfactory system of *Drosophila*, I wanted to focus on a more restricted area to examine the chloride responses in a particular glomerulus. I chose the DM2 glomerulus which is well characterized in the literature with regard to the excitatory information pathways (PELZ et al., 2006). It is innervated by OSNs expressing the OR22a which is known to perceive mostly general fruit odors in a diverse spectrum (HALLEM & CARLSON, 2006). Because of the already well known excitatory functionalities, OR22a represents an adequate research object with regard to the inhibitory signaling and especially its integration in the complex olfactory framework.

Like with the OR83b lines we started the characterization of OR22a with an analysis of the odor evoked chloride signals at the peripheral sensory level, the antenna. The ab3 sensillae which house the OR22a OSNs are located on the posterior side of the funiculus (FISHILEVICH et al., 2005). It was possible to see the clomeleon fluorescence in the cell bodies through the whole funicular volume from the anterior side. However, to allow for a more precise imaging I measured the antenna from posterior by erecting it. After doing so, one can clearly see the area with the ab3 sensillae in Figure 21A and also the region where the coordinate was placed for the imaging analysis. The kinetics in Figure 21B are very uniformly in slope and temporal characteristics but the varying amplitude and differing latency give a chance to distinguish between them. *Methyl hexanoate* evoked the fastest clomeleon response with the strongest amplitude which has the same intensity as the response to *ethyl-3-hydroxy butyrate* but with a different latency. The application of *benzaldehyde* and *pentyl acetate* resulted in two identical kinetics regarding slope and amplitude. The signal evoked by *1-hexanol* showed the weakest and slowest time course. In conclusion one can say that already on the antenna odors evoked specific clomeleon signals with distinct kinetics.

The next step was to measure the chloride signals one step further in the antennal lobe and to analyze if the signals were modified already on the primary sensory level. Fortunately the DM2 glomerulus lies dorsally and it was easy to see and to image this area using the described dissection procedure (Figure 22A). Also apparent was the set of OSNs deriving from the antennal nerve and guiding in a curve around the antennal lobe to synapse with the LNs and PNs within the glomerulus. Moreover, the antennal commissure which connects

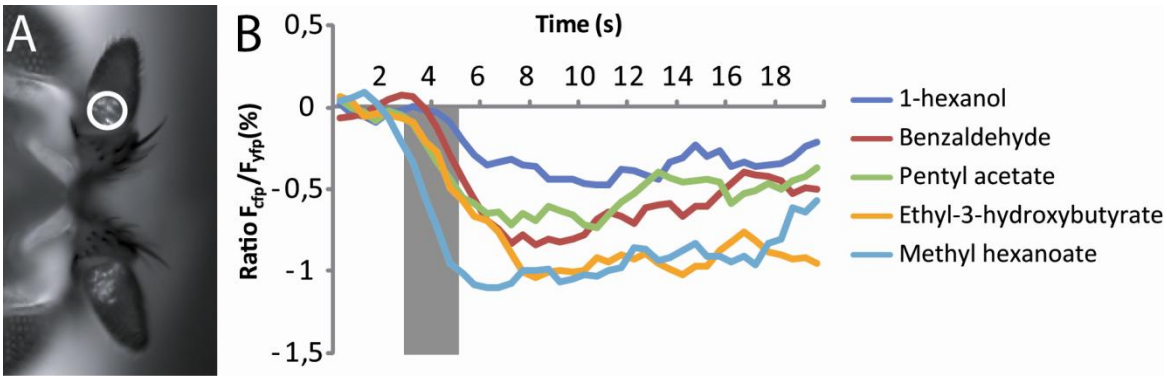

Figure 21. Odor dependent clomeleon kinetics on the antenna.
(A) Morphological view on the posterior side of the funiculus of an OR22a-GAL4:UAS-clomeleon fly. **(B)** Odor evoked clomeleon signals imaged from the sensillar region marked in A. The grey bar indicates the odor stimulus for 2s. Data are represented as median values (n = 8).

the two DM2 glomeruli in each antennal lobe was also clearly visible (Arrowheads in Figure 22A). Figure 22B shows the false color coded chloride signals as an overlay onto the morphological view. One can already see that *methyl hexanoate* evoked the strongest signal (Figure 22C). The odor which elicited the second strongest signal of almost 3% in the experiments was *isoamylacetate*, a banana component which was not shown on the antenna. The remaining three tested odorants *ethyl-3-hydroxy butyrate*, *1-hexanol* and *benzaldehyde*, elicited a significantly weaker clomeleon signal. These compounds evoked only very low chloride signals in the antennal lobe (around 1% fluorescence ratio change) which resembled their antennal signals. However, this is contrary to *methyl hexanoate* since this odor evoked a response of 1% fluorescence change on the antenna and up to 6% within the antennal lobe. Thus there has to be some mechanism like a presynaptic lateral input via LNs which is responsible for such a processing within a single neuronal level.

The results show that different odors evoked different chloride dependent signals in OSNs expressing the same OR. This equals the properties of excitation which also showed different odor specific dynamics within a particular OSN population. This was already shown before (PELZ et al., 2006) but in order to have comparable data with the clomeleon signals I tested the odor set again with OR22a-GAL4:UAS-cameleon flies. Using cameleon I could image the intracellular calcium concentration changes induced by odors under the identical conditions and in the same glomerulus as applied for the clomeleon imaging. These data are shown in Figure 23 in direct comparison with the chloride dependent responses.

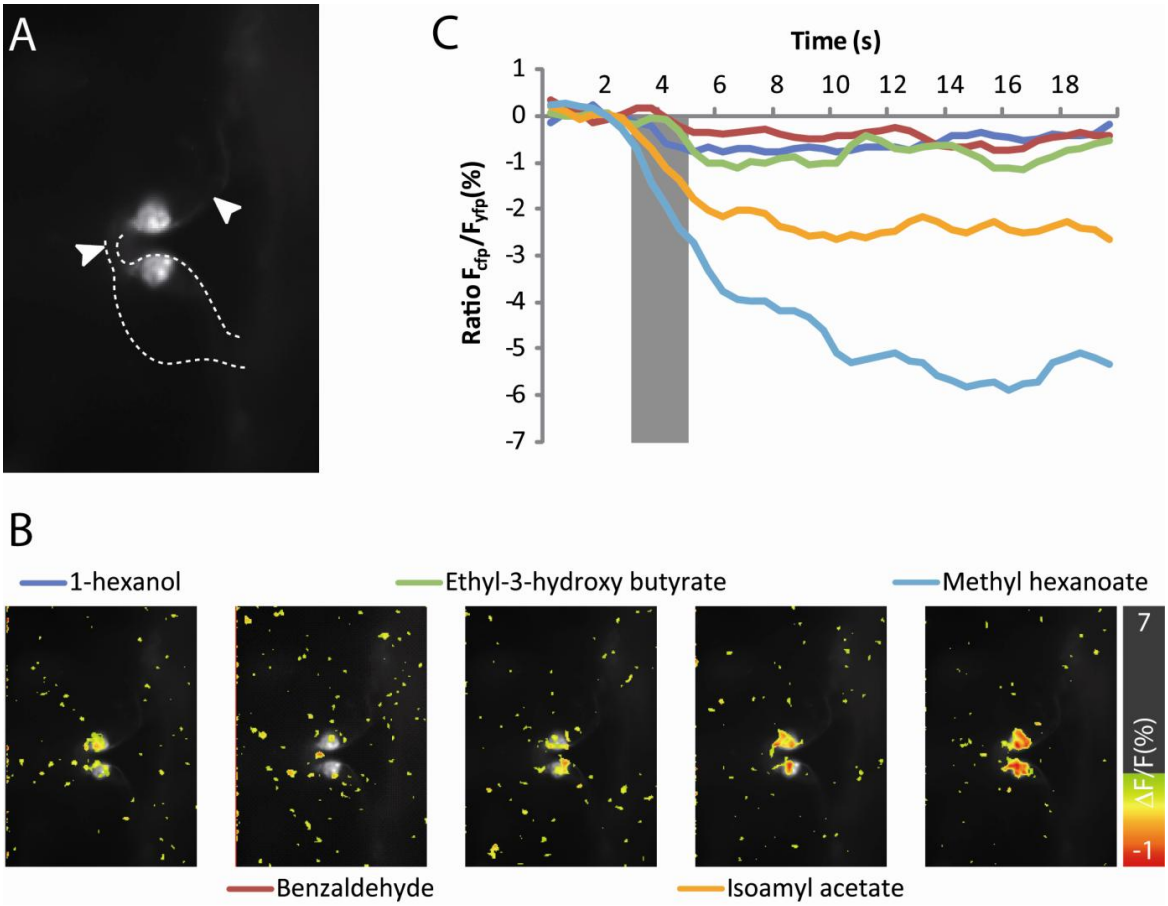

Figure 22. Odor dependent clomeleon kinetics in a single glomerulus in the antennal lobe.
(A) Morphological view of the DM2 glomerulus innervated by OSNs expressing OR22a (OR22a-GAL4:UAS-cameleon). **(B)** Morphological views of single odor runs with a false color coded overlay of the elicited clomeleon signals. **(C)** The corresponding kinetics to the examples shown in B. The grey bar indicates the odor stimulus for 2s. Data are presented as median values (n = 6).

Interestingly, the spectrum of calcium signals is much more diverse in the DM2 glomerulus compared to the very restricted chloride related ones. The cameleon signals displayed a great variety of amplitude, slope and duration. For example, the responses to *1-hexanol*, *ethyl benzoate* and *ethyl-3-hydroxy butyrate* showed an initial peak with a short latency. The signal decreased after stimulus offset, but did not return to baseline until the end of the measurement. Measured with clomeleon these odors elicited only a very small signal (e.g. *ethyl-3-hydroxy butyrate* and *1-hexanol*) or no signal at all (e.g. *ethyl benzoate*). Other compounds as *benzaldehyde* and *anisole* did also not evoke a clear chloride signal in the OR22a neurons but showed a moderate calcium response with cameleon, after stimulus offset, which was very pronounced for *anisole*. It is most interesting that the two odors that elicited the strongest excitatory signals, namely *isoamylacetate* and *methyl hexanoate*, also

evoked the strongest chloride signals. Furthermore, these two odors displayed a very specific time course with a plateau without a clear recovery until the end of the measurement which again represents a similarity to the clomeleon kinetics. The partly correlation of cameleon and clomeleon signals to several odors on the one hand and the total divergence regarding other tested compounds on the other hand gives a hint on the processing network effects taking place in the antennal lobe. Furthermore it seems that excitation and inhibition are treated differently and might influence each other in a very complex way. To see if this disparity and simultaneous synchrony of calcium and chloride signals holds also true for the whole receptor repertoire or if this is a specific phenomenon of the OR22a OSNs in the antennal lobe I had to analyze it more profoundly.

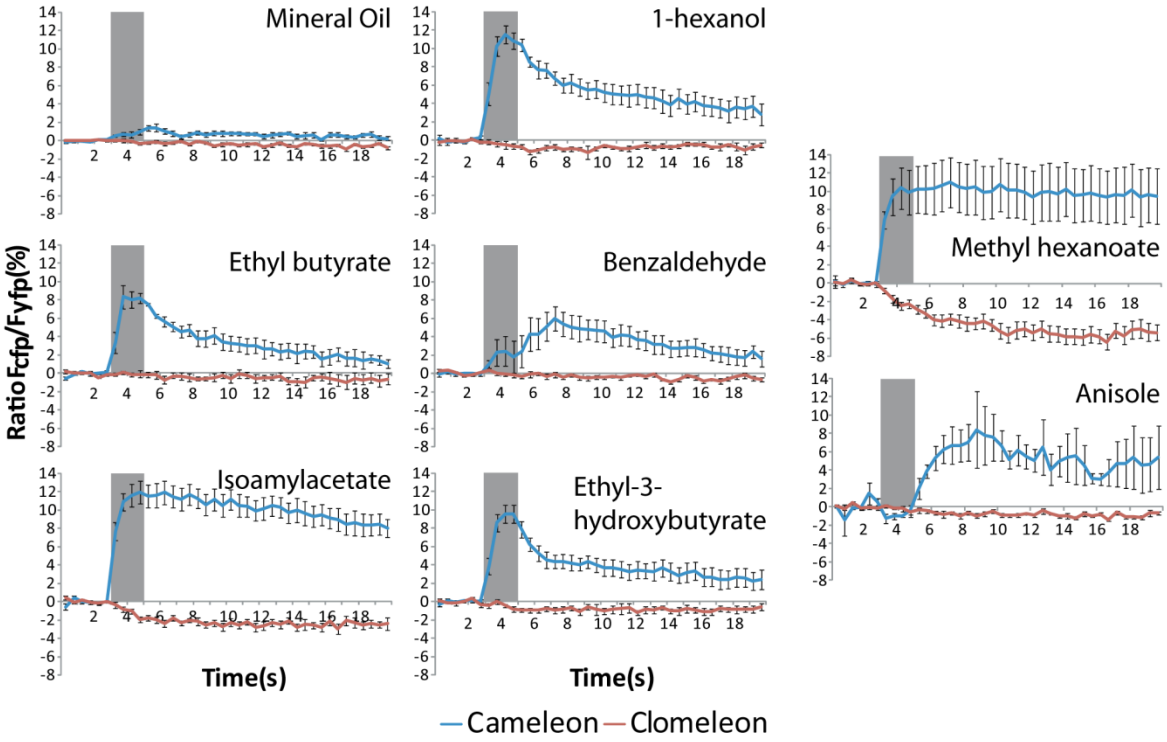

Figure 23. Cameleon and clomeleon signals in the DM2 glomerulus.
Cameleon and clomeleon signals evoked by the same odors measured in OR22a-GAL4:UAS-cameleon or -clomeleon flies. The application of the odor takes place after 3 seconds and lasts for 2 seconds indicated by the grey bar. Data are presented as median ± SEM (n= 6-12).

3.8. Comparison between the antennal and antennal lobe signals

After describing the clomeleon responses on the antenna and in the antennal lobe as well as the comparisons with the cameleon signals, I was interested in analyzing the calcium responses also on the antenna. Therefore I used again the OR22a-GAL4:UAS-cameleon flies to complete the signal set with the calcium responses from the dendrites and cell bodies of the labeled OSNs on the antenna. Figure 24 shows the entire normalized OR22a signals separated into cameleon (A) and clomeleon (B) signals measured on the antenna (blue) and within the antennal lobe (red). Interestingly, the calcium signals were almost identical on the antenna and in the antennal lobe displaying no presynaptic lateral processing within the primary reception level of the OSNs. The odor evoked calcium signals seem to be forwarded without any significant modulation in the DM2 glomerulus. Some odorants like *ethyl benzoate* and *1-hexanol* tend to cause stronger excitatory calcium signals in the antennal lobe than on the antenna. I did not observe any kind of calcium signal reduction along the OSNs. Most of the odors showed similar signal intensities between antenna and antennal lobe.

Regarding the odor signals reported by clomeleon (Figure 24B) I observed a chloride signal shift from the antenna to the antennal lobe within the OR22a OSNs. The most significant shift could be observed for the chloride signals induced by *benzaldehyde* and *ethyl-3-hydroxy butyrate*. These two odors evoked the strongest inhibitory signals on the antenna following *methyl hexanoate*. Interestingly, in the antennal lobe both odors elicited very low chloride currents. *Benzaldehyde* and *ethyl-3-hydroxy butyrate* showed the same antennal lobe signals as mineral oil. *Ethyl benzoate* and *1-hexanol* already evoked only low signals on the antenna and these were even lower in the antennal lobe although the shift is not significant. For *isoamylacetate* it actually seems as there is a little increase regarding the inhibitory signaling in the antennal lobe compared to the antennal ones but also without significance. Outstanding in any case is the constancy exhibited by the *methyl hexanoate* signals. Regardless if I imaged the antenna or the antennal lobe, *methyl hexanoate* elicited the strongest chloride increase in the OR22a OSNs.

These contradictory results concerning the signal processing along the OSNs might indicate that the measured calcium and chloride ion currents underlie different processing mechanisms on their way from the periphery to the first olfactory center in the central

nervous system. How this could be accomplished remains unclear for the moment and needs further experiments.

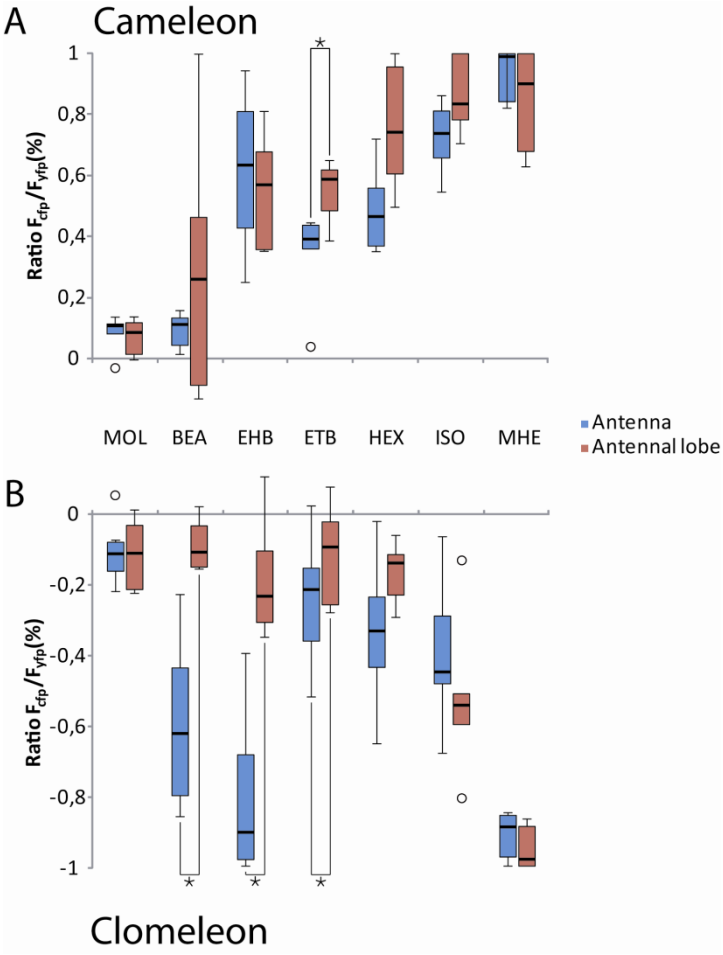

Figure 24. Comparison of the calcium- and chloride signals between the antenna and the antennal lobe.
(A) Cameleon signals to different odors on the antenna and within the antennal lobe (n = 6). **(B)** Comparison of the clomeleon signals between antenna and antennal lobe (n = 6 - 8).

3.9. Modulatory effects of single odors

During the imaging measurements with the OR22a-GAL4:UAS-cameleon flies I observed that several odors change the characteristics and intensity of their calcium signals drastically during the measurement, while others did not. This led me to the assumption that one of the odors might be somehow capable of modulating signals evoked by other odors. To verify this I first had to find out which one of the odors could be responsible for this effect or if it is a summed interaction effect of several odors. Since most of the tested odorants like *ethyl-3-hydroxy butyrate*, *1-hexanol*, *ethyl benzoate*, *benzaldehyde* and *isoamylacetate* are established compounds in olfactory research and are not known to elicit modulatory effects I ruled them out. However, additional to these "traditional" odors I used three new odors. These were *γ-valerolactone*, *anisole* and *methyl hexanoate*. The former two odors were selected especially because they evoked a negative calcium signal at high concentration in the OR22a-GAL4:UAS-cameleon flies studied by Daniela Pelz (PELZ et al., 2006). I was curious to see if these two odors also have an effect on the chloride concentration. The latter odor, *methyl hexanoate*, was shown to be the best known ligand for the olfactory receptor 22a (PELZ et al., 2006). After testing the different possible odor constellations I ruled out *γ-valerolactone* and *anisole* and identified *methyl hexanoate* as the responsible odor that affected the calcium responses to other odors. One can see in Figure 25B that the calcium responses in the antennal lobe to all measured odors changed drastically after the first application of *methyl hexanoate*. The previous positive signals indicating a calcium influx switched to a negative calcium signal after the application of *methyl hexanoate* now representing an efflux of intracellular calcium ions. This potential modulation could be observed in the OR22a-GAL4:UAS-cameleon flies in the DM2 glomerulus but not in the corresponding sensillae on the antenna (Figure 25A). This interesting aspect of the phenomenon as taking place exclusively in the antennal lobe while it cannot be observed on the antenna might give me a new example to explore the functionalities of the intrinsic processing mechanisms of the antennal lobe. Possibly this modulatory effect is related to an influence on the chloride ion concentration changes. To test this I measured the same odor sequence in the OR22a-GAL4:UAS-clomeleon flies. As Figure 25C shows the *methyl hexanoate* application did not affect the chloride signals to other odors on the antenna which corresponds to the observation of the calcium signals. Also within the antennal lobe

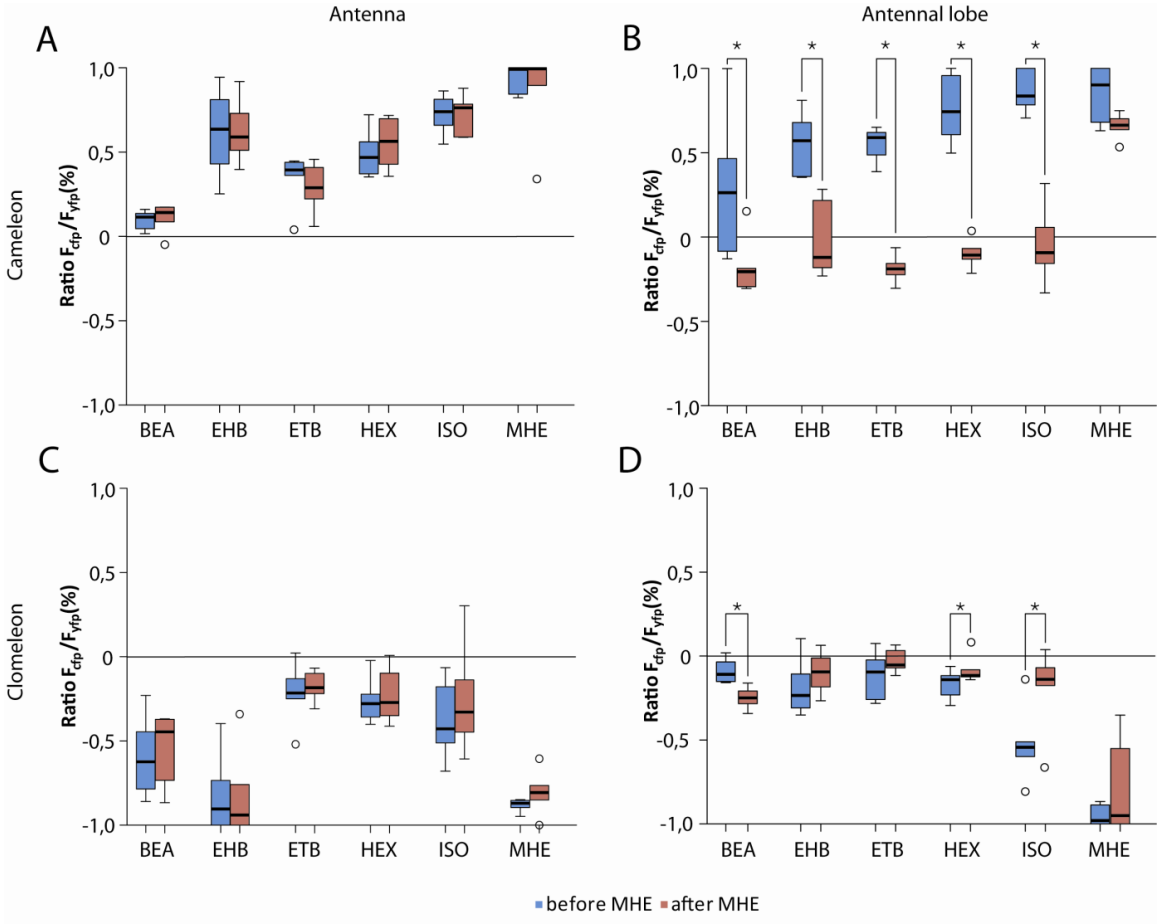

Figure 25. Effect of *methyl hexanoate* application on the calcium- and chloride signals on the antenna and in the antennal lobe.
(A) Calcium signal before and after the application of *methyl hexanoate* on the antenna **(B)** and in the DM2 glomerulus. **(C)** The corresponding chloride signals on the antenna **(D)** and in the DM2 glomerulus (n = 6).

such a general modulation could not be observed as it was taking place during the calcium measurements (Figure 25D). Only some odors like *benzaldehyde*, *1-hexanol* and *isoamylacetate* displayed a modulatory effect induced by *methyl hexanoate* but by far not as strong as the observed calcium signal modulation. *Ethyl-3-hydroxy butyrate*, *ethyl benzoate* and *methyl hexanoate* itself were completely unmodified before and after the *methyl hexanoate* treatment.

In order to analyze the exact functionality of this mechanism I wanted to know if the effect is linked to *methyl hexanoate* itself and its unique interaction with the olfactory receptor 22a or if the coarse chemical structure is capable to provoke the modulation. Therefore I tested the effect of *ethyl hexanoate* application, known as the second best ligand for OR22a (PELZ et al., 2006). I observed the same effect at least for *1-hexanol*, *benzaldehyde*, *isoamylacetate*

and *ethyl-3-hydroxy butyrate* (Figure 26). The odor applications elicited a positive calcium signal in the DM2 glomerulus (Figure 26A), which was shifted to a negative calcium current after the treatment with *ethyl hexanoate* (Figure 26B). The effect was almost identical to the one evoked by *methyl hexanoate* except that *benzaldehyde* did not show such a strong shift. Since I did not observe this modulatory effect provoked by any of the other odors the two hexanoates are solely responsible for it so far.

Next I analyzed if this modulation is odor concentration dependent. Since the application of high odor concentrations (as 10^{-1}) is often an issue because they are discussed to be artificial and might derange the olfactory perception, I had to test if the effect is caused by high odor concentration. Thus I tested lower concentrations of *methyl hexanoate*, as 10^{-5} and 10^{-3}, in addition to the 10^{-1} concentration to see if there is a gradual effect correlated to the concentration (Figure 26). A dose-dependent effect could clearly be observed for the *methyl hexanoate* calcium signals shown in Figure 27A. Although the slope and signal duration remained roughly constant during the measurement, the amplitude increased with rising

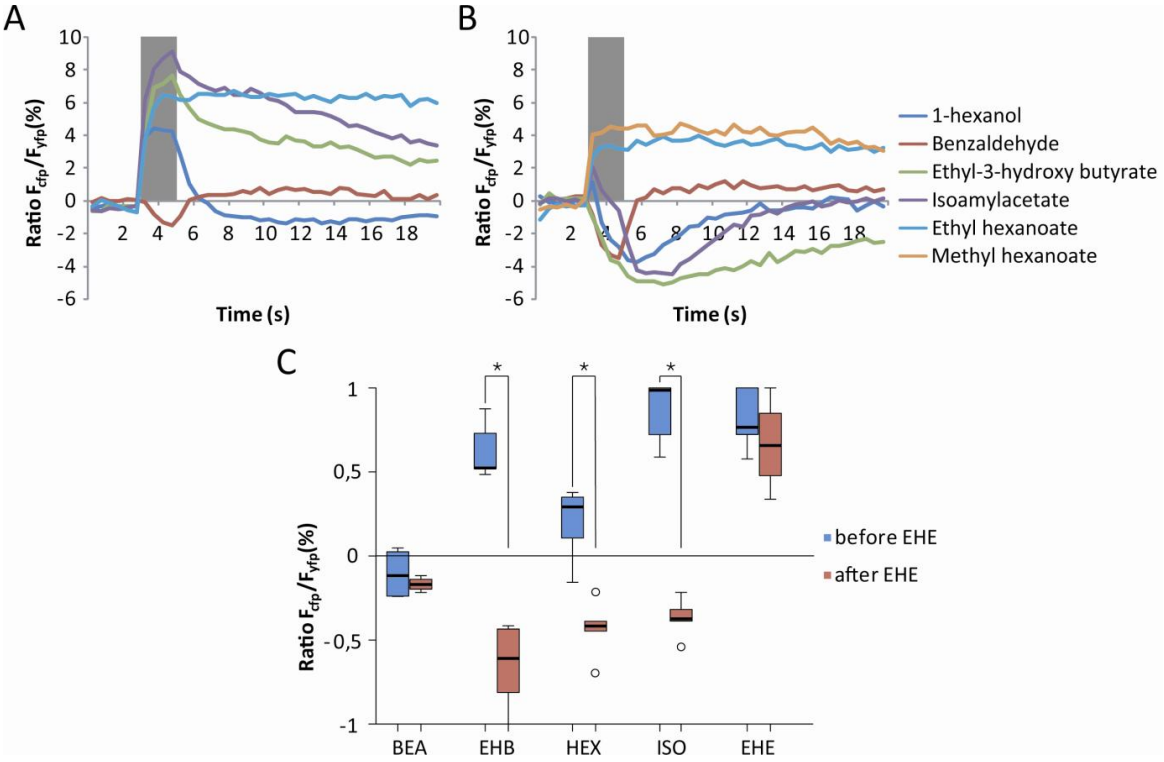

Figure 26.Modulatory effect of *ethyl hexanoate* in the DM2 glomerulus.
(A) Odor specific calcium signals in glomerulus DM2 prior to the application of *ethyl hexanoate*. **(B)** Modulated calcium signals after the application of *ethyl hexanoate* (n = 4-5). **(C)** The normalized calcium signals of the complete experiment represented as box plots (n = 4-5). The grey bar indicates the odor stimulus for 2s. (A, B) Data are represented as median.

concentration from 10^{-5} up to 10^{-1}. Furthermore the odor related calcium signals displayed a clearly gradual decrease of excitatory signal strength with increasing concentration of *methyl hexanoate* (Figure 27B). However, the signal switch induced by *methyl hexanoate* was not as strong as when I directly applied a concentration of 10^{-1}. 1-hexanol and *ethyl-3-hydroxy butyrate* descended stepwise from their initial positive calcium signal to a clearly negative one after the application of the 10^{-3} and 10^{-1} concentration of *methyl hexanoate*. Furthermore *isoamylacetate* was gradually approaching the base line with increasing *methyl hexanoate* concentration. *Benzaldehyde* did not change from its initially evoked slightly negative signal in contrast to the other odors. In summary one can say that the modulation of the odor evoked calcium signals underlies a dose response effect which causes a gradual decrease with a possible adaption of single odors to the observed *methyl hexanoate* effect.

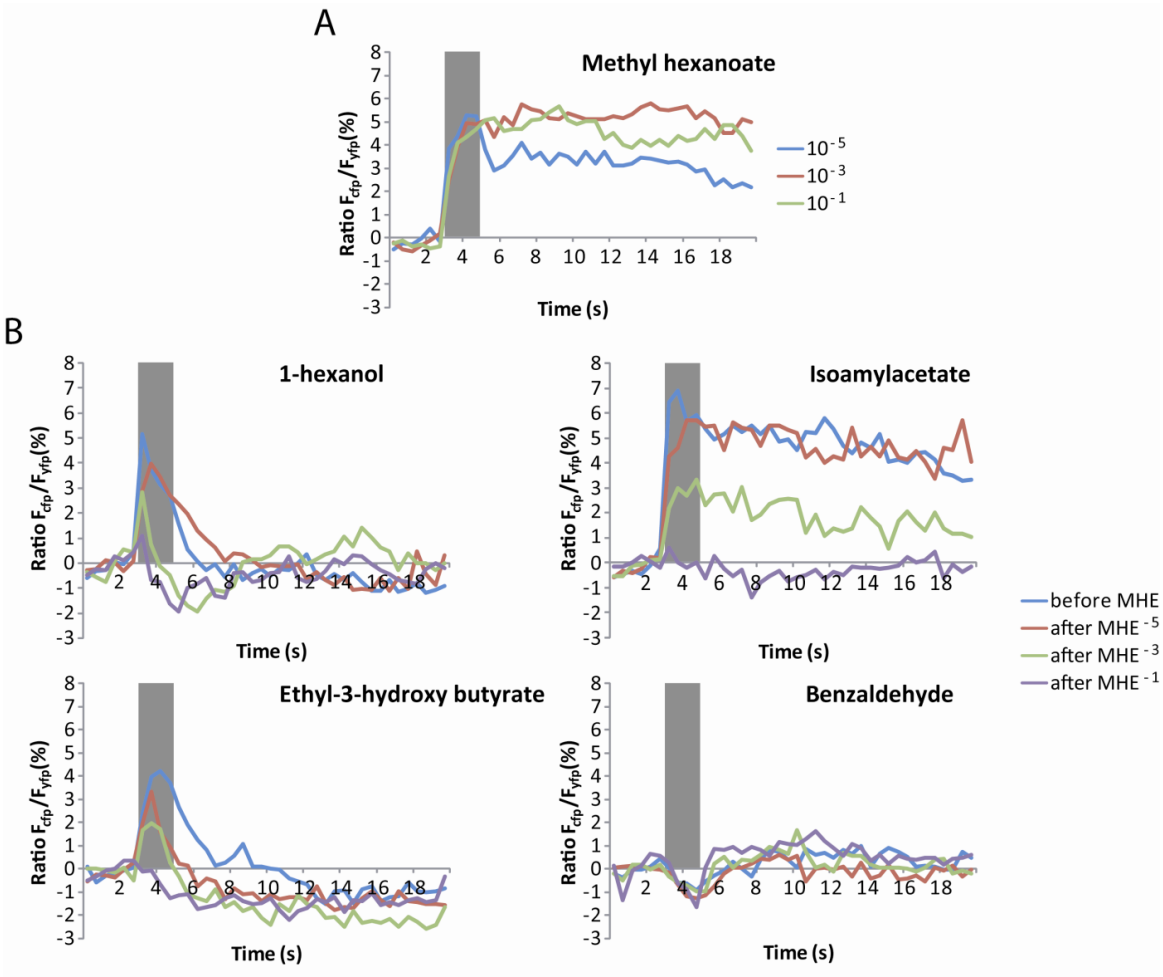

Figure 27.Influence of the *methyl hexanoate* concentration on the signal modulation.
(A) Calcium signals evoked by *methyl hexanoate* with rising concentration from 10^{-5} up to 10^{-1} (n = 3). **(B)** Gradual effect of an increasing concentration of *methyl hexanoate* on the application of several odors (n = 5). The grey bar indicates the odor stimulus for 2s. Data are represented as median.

It is difficult to identify the exact origin of the phenomenon since it occurs within the OSN set only at the terminating axons in the antennal lobe. But with this information it is obvious that the processing has to take place at the presynaptic sites in the antennal lobe since no signal manipulating mechanisms are known within the antennal nerve so far. This could mean that some other glomeruli beside the DM2 are also activated by the *methyl hexanoate* and somehow influence the response to the other odors by OR22a. In order to analyze if the modulatory effect is restricted to the OSNs expressing OR22a or if it arises from other OSNs, I tested the effect in OR83b-GAL4:UAS-cameleon flies. This experiment will give a hint if any of the other visible glomeruli is similarly affected by the treatment with *methyl hexanoate* as DM2 does and if so, whether this can be responsible for the phenomenon in the DM2 glomerulus. Unfortunately Figure 28 shows that none of the imaged glomeruli labeled by the OR83b GAL4 line elicited such a general calcium signal modulation to *methyl hexanoate* as DM2. Indeed some of the glomeruli exhibit a sparse modulation because of the *methyl hexanoate* application but mostly only to single odorants. Thus it seems that the general effect is restricted to the OR22a OSN population. Since the DM2 glomerulus is located in a slightly deeper layer of the antennal lobe it is not so easy to see in every specimen of the OR83b flies. The odor related calcium signals are a little bit covered by neighboring or overlaying glomeruli especially when they also respond to the tested odors like the DM6 in particular. Because of this, calcium signals in the DM2 are just reduced after the treatment but not reversed as in the OR22a-GAL4:UAS-cameleon measurements. Further did *ethyl benzoate* elicit a stronger inhibitory signal in the DL1 glomerulus after the *methyl hexanoate* application. The DM5 glomerulus displayed a decreased calcium response to *pentyl acetate* as well as a negative one to *ethyl benzoate* after *methyl hexanoate* application. In addition the VM5 and DM6 glomeruli lose calcium signal strength to *pentyl acetate* after the *methyl hexanoate* application.

To illustrate the signal shift once more in the OR83b glomeruli set, I separated the responses in the DM2 glomerulus from the responses in the surrounding ones (Figure 29). Using the box plot representation the significant signal shift of the single odor pairs is still evident in DM2 even with the diffused emission light of the adjacent glomeruli.

Although not completely deciphered the described modulatory effect potentially gives us a new tool to examine the functionalities of lateral input delivered by LNs or other so far unknown mechanisms (TURNER & RAY, 2009).

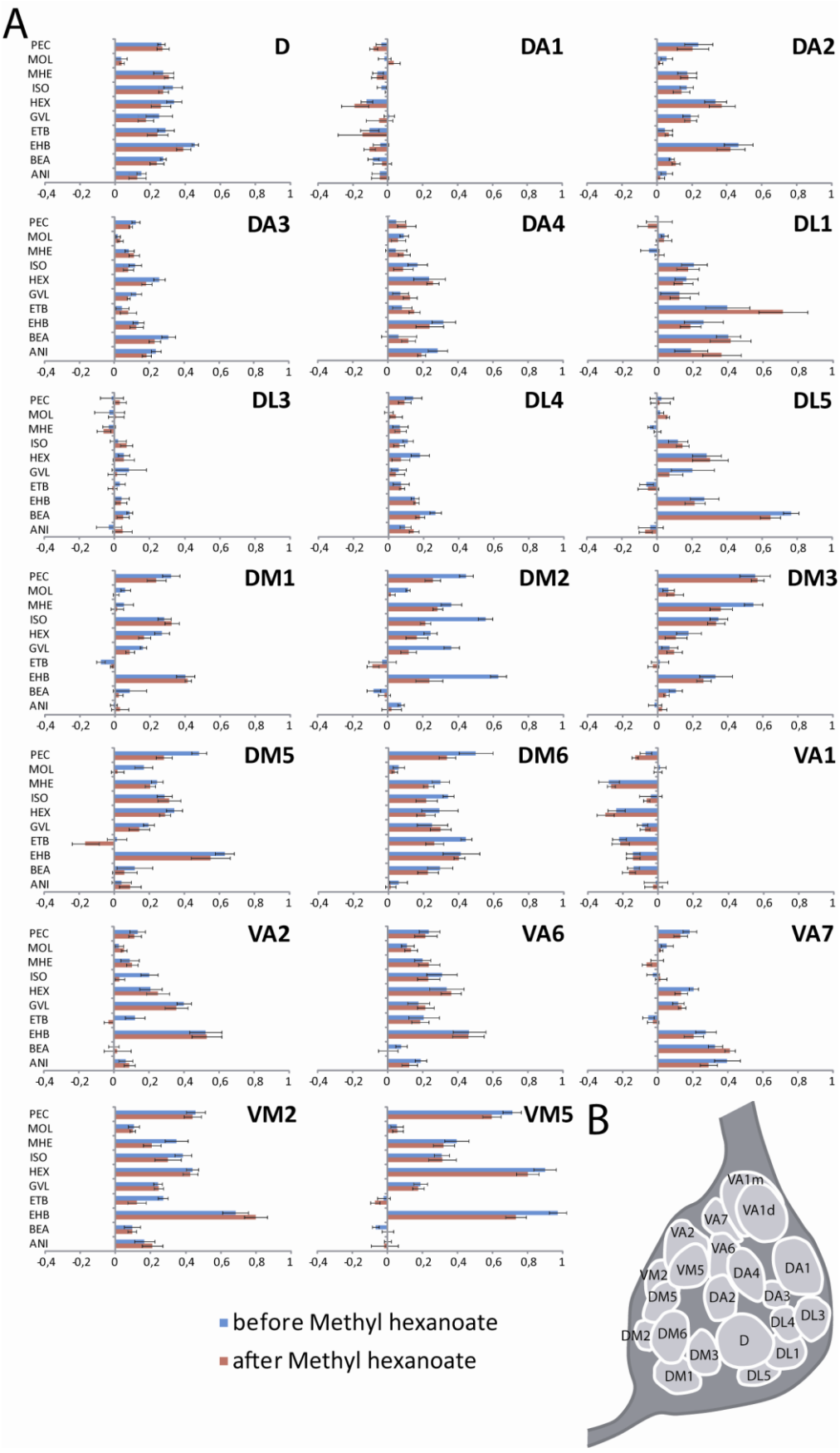

Figure 28. Effect of *methyl hexanoate* application on odor responses in OSNs in the antennal lobe. **(A)** Only DM2 shows the modulatory effect after the application of *methyl hexanoate* (n = 5). **(B)** The glomerular map based on the 3D-reconstruction in AMIRA.

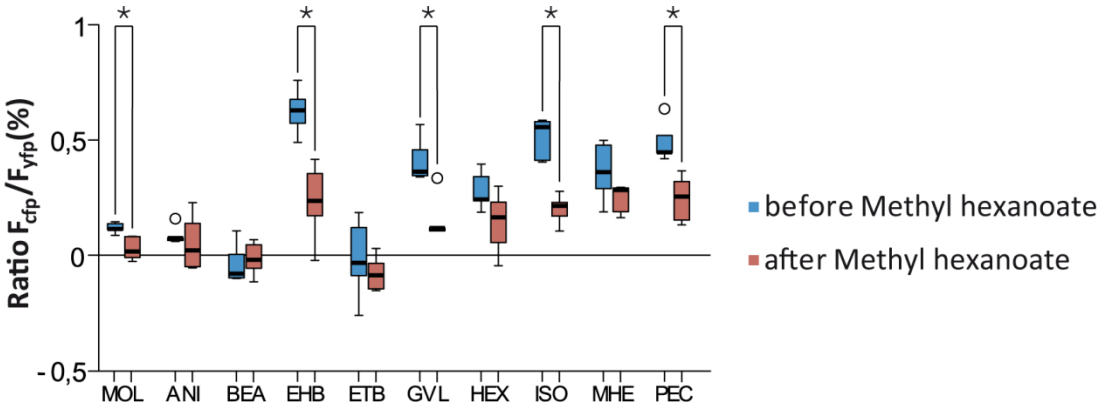

Figure 29. Extracted normalized DM2 calcium signals from the OR83b measurement in Figure 28 represented as box plots.

The normalized odor signal pairs are separated in the signal before (blue) and after (red) the treatment with *methyl hexanoate* (n = 5; *p<0.05).

4. Discussion

The main goal of this thesis was to introduce clomeleon as a genetically engineered indicator for chloride ions in *Drosophila melanogaster*. Furthermore this indicator should be used to examine the chloride related inhibitory pathway at the first olfactory processing level, the antennal lobe. Therefore I analyzed the intracellular chloride concentration changes on the antenna and within the antennal lobe evoked by the application of single odorants. To achieve this I used transgenic flies that expressed the chloride sensitive protein clomeleon in OSN (i.e. OR83b driver) and PN (i.e. GH146 driver) populations using the GAL4:UAS transcriptional system. In addition I imaged a glomerulus-specific subpopulation of about 30 OSNs expressing a single OR (OR22a) by expressing clomeleon selectively in these neurons. In this way it was at first possible to image the overall chloride signal pattern in the olfactory system. Second, I analyzed how the inhibition interacted with the excitation by using cameleon to image odor-evoked calcium responses in the same neuronal populations. Third, I described the intraglomerluar discrimination of single odors by chloride currents. Furthermore the transfer of inhibitory signals from the OSN to the PN level was analyzed showing distinct pattern differences between the processing levels.

During these experiments I observed a phenomenon where a high concentrated single odor modulated the calcium, partly also the chloride signals, of other odors within one glomerulus. Furthermore I applied and further developed a method to generate reconstructions of glomerular neuropiles in combination with immunostaining and *in vivo* confocal stacks.

4.1. Determination of the identity of the measured clomeleon signals

At first I could show that clomeleon (KUNER & AUGUSTINE, 2000), under the control of a tissue specific GAL4 driver, is able to report intracellular chloride currents in a specific neuronal set. Long time this imaging technique was restricted to calcium sensitive sensors like cameleon (MIYAWAKI et al., 1997; FIALA& SPALL, 2003; PELZ et al., 2006) or G-CaMP (DACKS et al., 2009; SILBERING et al., 2008) and therefore the main focus was to describe only the excitatory tasks of neuronal systems (MIESENBÖCK et al., 2001). Although inhibition was

long time neglected besides excitation, it has received more attention during the last years (STOPFER, 2005; WILSON & LAURENT, 2005; OLSEN & WILSON, 2008; ROOT et al., 2008) together with the properties of synaptic and non-synaptic chloride channels (WICHER et al., 2001). It is apparent that inhibition plays a role in the reception and transmission of information in the olfactory system of *Drosophila melanogaster*.

The initial control experiment with potassium gluconate (Figure 11) showed that clomeleon is able to report chloride changes at the input (OSNs) as well as the output (PNs) level of the antennal lobe. The application of potassium gluconate increased the intracellular potassium concentration throughout the antennal lobe neurons (KACZOROWSKI et al., 2007) by passing through their open potassium channels leading to the excitation of all neurons. The measured fluorescence decrease indicates an increase of the intracellular chloride concentration due to the functionality of clomeleon as a chloride indicator (KUNER & AUGUSTINE, 2000). A potential origin for this chloride responses are the LNs with their GABAergic presynaptic connections to the OSNs and the postsynaptic ones to the PNs (OKADA et al., 2009). To identify the responsible neurotransmitter I applied GABA onto the brain of the same fly lines and discovered a strong clomeleon signal, too (Figure 12). Indeed GABAergic LNs have been identified in *Drosophila* adults (WILSON et al. R. , 2005), larvae (PYTHON & STOCKER, 2002) and other insect species (HOSKINS et al., 1986; MALUN, 1991; LEITCH & LAURENT, 1996; BICKER, 1999). Since GABA itself has a bigger molecular weight than potassium gluconate in solution it diffused potentially slower and therefore evoked a flat chloride decrease in the beginning. After a while it activated more and more GABA receptors and the clomeleon response became steeper eliciting a biphasic response. It is not clear if this response underlies a threshold. Since the kinetics of OSNs as well as PNs became steeper as the time trace of the clomeleon signal reached a decrease of 5% it appears possible. Next I identified the contribution of the different GABA receptor types to the measured GABA induced clomeleon signals. $GABA_B$-type receptors have been identified for the OSNs (ROOT et al., 2008) as well as for the PNs of the antennal lobe glomeruli together with $GABA_A$-type receptors (HARRISON, et al., 1996; OLSEN & WILSON, 2008; OKADA et al., 2009). The two GABA antagonists CGP54626 and PTX lowered the imaged chloride responses by reducing the inhibitory chloride currents in OSNs, LNs and PNs (WILSON et al., 2005). PTX binds to the $GABA_A$-type receptors and therefore directly diminishes the chloride influx in PNs (Figure 20A). Additional to the presynaptic $GABA_B$-type receptors (ROOT et al., 2008) I

confirmed that they also exist at the post synapse of PNs since CGP54626 reduced their clomeleon responses in PNs (Figure 20C). It is known that the $GABA_B$-type receptors, which are metabotropic receptors (BAZHENOV et al., 2001), directly affect intracellular calcium concentrations by causing a decrease if activated (HAMASAKA et al., 2005) but it is not clear if they affect chloride currents in insects, too. My results provide evidence that $GABA_B$-type receptors are involved in the odor induced chloride response since the specific blocker CGP54626 significantly reduced the regarding signals.

In addition the recordings of odor evoked clomeleon signals already on the antenna (Figure 14) indicate that the specific ORs expressed in the OSNs directly influence the dendritic chloride concentration. This could be realized due to the presence of voltage gated chloride channels in the OSN dendrites (WICHER et al., 2001). These channels would be activated by action potentials and lead to a downsizing of strong excitatory odor responses since these would provoke a stronger chloride influx. Therefore high concentrated odors, along with low concentrated ones, in natural occurring blends could not cover the weaker odors in order not to lose olfactory information. This primary processing would add up with the potential interaction of single odors with several receptors to modify their response properties and therefore shape typical blend response patterns (OKA et al., 2004; DUCHAMP-VIRET et al., 2003).

The pH sensitivity of CFP/YFP based sensors is often an argument since the changing intra- and extracellular ion concentrations are accompanied by a pH change. It has been shown that a pH shift of 0.2 units at a chloride concentration of 150mM has a strong influence on the chloride sensitivity of the purified clomeleon protein (KUNER & AUGUSTINE, 2000). The chloride concentration in the hemolymph of *Drosophila* is approximately 150mM. However, it has been shown that a pH change of up to 0.5 units, induced through saline exchange, does not affect the clomeleon fluorescence in the OSNs significantly (FIEDLER, unpublished Data).

4.2. Temporal resolution of clomeleon responses

Regarding the temporal properties of the measured chloride responses, I measured an interval of 100s that was needed for the clomeleon signals to return to the initial baseline

(Figure 13). At first this seems extremely long since most neuronal events last only for a few milliseconds. However, the important difference of inhibitory responses compared with excitatory ones is that the inhibitory ones do not spike (HAMASAKA et al., 2005; TURNER & RAY, 2009). Action potentials always elicit a spiking response in electrophysiology which demands fast ion in- and efflux. However, a hyperpolarization is a solitary event, lasting over a longer period (WILSON et al., 2004b). Therefore it is possible that the long lasting increase of the intracellular chloride concentration is not an artifact of the fluorophores kinetic. As one can see the fast decay at the beginning of the chloride signals (Figure 13) and the similar fast recovery of the fluorescence after very short artificial signals (KUNER & AUGUSTINE, 2000), it is clear that the kinetic of clomeleon allows it to report faster intracellular chloride changes if present.

In conclusion one can say that clomeleon reports long-lasting chloride signals in OSNs and PNs that have an excitatory origin, are GABA related over $GABA_A$- and $GABA_B$-type receptors and potentially indicate inhibitory tasks.

4.3. Transmission of clomeleon signals through the olfactory system

With the specified clomeleon functions I imaged the spatiotemporal distribution of chloride dependent inhibitions throughout the first processing level of the olfactory system. Primary I showed that the antennal chloride signals in response to odor stimuli are uniformly spread over the coarsely separated sensillar fields (Figure 14C). They did not elicit a spatial pattern as it is known for excitation on the antenna (de BRUYNE et al., 2001) but a temporal one. Some odors displayed a short negative response, while other odors induced a strong and long-lasting response over the whole measurement. This could mean that the initial voltage gated inhibitory signals at the periphery are unspecific regarding the identity of the odor since all sensillae responded in the same way. Nevertheless the different odors could be distinguished by eliciting a temporally different chloride signal all over the funiculus. Furthermore the measured signals only occurred at high odor concentrations of 10^{-1} which evoked strong excitatory signals and therefore probably indirectly contributed to the higher inhibitory chloride currents through voltage gated channels. This again could be a mechanism of downsizing the strong excitatory signals and therefore retain a better

sensitivity to dissect a complex blend into its single components. Another reason could be that these odors at such high concentrations become behaviorally repellent themselves which would be reflected in a direct inhibitory perception. However, this hypothesis has to be tested in a behavioral assay. The literature notes the possibility of a direct crosstalk between adjacent OSNs within one sensillum (DOBRITSA et al., 2003). A technical problem of clomeleon at the momentary state is the signal-to-noise ratio which is not optimal and therefore makes it often difficult to distinguish sole movement artifacts from the actual signal (Figure 14C). With the time this problem will hopefully be solved with improved versions of clomeleon.

Additional to the antenna I could also image the axonal terminals of the OSNs in the antennal lobe (Figure 16). The spatiotemporal glomerular patterns were more odor specific than on the antenna as every odor evoked a unique pattern of glomerular inhibitions (Figure 18). Among the patterns several different types could be observed: A single odorant could elicit a broad and intermediately strong signal pattern (*benzaldehyde* and *ethyl benzoate*), a very sparse one affecting single glomeruli (11-*cis vaccenyl acetate*), a broad one where a few glomeruli stuck out (*pentyl acetate*, *isoamylacetate* and *1-hexanol*) or the chloride responses were restricted to an area where all glomeruli showed strong inhibitory responses (*ethyl-3-hydroxy butyrate*). These patterns did not reflect the uniform antennal signaling of the OSNs. Since the sensillae housing a specific OR are spread over a wide area of the funiculus and mix with each other (VOSSHALL et al., 1999; FISHILEVICH & VOSSHALL, 2005), one would not expect to observe a precise antennal pattern when multiple ORs are affected. Furthermore one has to admit that the dendritic signals are supposed to be pure with potentially no processing (OKA et al., 2004), while the axonal ones should underlie already presynaptic input (ROOT et al., 2008) and therefore underwent a first processing. What is even more challenging is the comparison of the OSN chloride responses with the PN ones. A direct relation is impossible since OSNs are not GABAergic (OKADA et al., 2009) and thus are unable to forward inhibition directly to the PNs (WILSON et al., 2004b). That could explain why the spatiotemporal chloride response patterns of PNs originate potentially from different glomeruli as those showing presynaptic inhibition in the OSNs. To forecast the PN signals it would be necessary to analyze the excitatory output of OSNs combined with the interglomerular network of the GABAergic LNs (WILSON & LAURENT, 2005). In addition the existence of the different GABA receptor types across the postsynapses of the whole PN population has to be identified and

taken into account. Although the exact origin of the postsynaptic glomerular chloride signals in PNs still remains unclear without the above mentioned information, a spatiotemporal chloride pattern is apparent (Figure 18C). A classification of the signal patterns is not as obvious as in the OSNs since most odors evoke a broad inhibitory pattern across the whole dorsal antennal lobe. This indicates a signal expansion of the excitation present in the OSNs probably through the GABAergic LNs since the tested odor concentrations already evoke a broad excitatory pattern in OSNs (Figure 28). Interestingly some of the odor evoked inhibitory patterns did not differ strongly between the processing levels (e.g. *pentyl acetate*, *isoamylacetate, ethyl benzoate* and *1-hexanol*) whereas other odors did (e.g. *benzaldehyde*, *ethyl-3-hydroxy butyrate* and *11-cis vaccenyl acetate*). This might imply that the GABAergic LNs receiving excitatory input through similar represented odors might form synapses onto OSNs and PNs within the same glomerulus. Furthermore the odors that evoked different inhibitory patterns in OSNs and PNs might excite inhibitory LNs that possess branches to a large set of OSNs and PNs in distinct glomeruli. This would in turn lead to a sharper excitatory pattern for the respective odor since lots of glomeruli would be inhibited by pre- and/or postsynaptic potentials. The less dissimilar pattern shift would then contribute to a broader excitatory tuning of the glomerular set.

4.4. OR22a as a case study of the chloride signal transmission

A more detailed view on the chloride concentration changes present in a specific neuronal population was obtained with the help of the OR22a-GAL4 line (VOSSHALL et al., 2000). Clomeleon reported odor specific chloride responses on the antenna (Figure 21B) whose slopes are uniform but differentiate between the odors by amplitude and latency. If these responses originate from voltage gated chloride channels (WICHER et al., 2001), as assumed above, they would correlate with the calcium responses in the same OSN which has to be tested.

The odor induced chloride responses in the antennal lobe resemble those imaged on the antenna (Figure 24). The strongest responses are evoked by the same odors as in the periphery but the odor separation appears more distinct, since the chloride response amplitudes in the antennal lobe exceed the antennal ones significantly. For example, *methyl*

hexanoate elicited still the strongest inhibitory response but the chloride response amplitude in the antennal lobe was twice as high as the one evoked by *ethyl-3-hydroxy butyrate*. This leads to an increased separation by scattering the inhibitory odor responses over a wider range and therefore to a diversified processing of the excitatory odor related input. Since the presynaptic chloride responses in the antennal lobe underlie GABAergic lateral input from the LNs, they are supposed to be stronger than on the antenna. In addition the relative chloride response intensity of the other odors tested decreased in the antennal lobe (Figure 24B). Since the chloride responses on the antenna potentially originate from voltage gated chloride channels, they are more uniform at the dendritic terminals as they receive no lateral input. This uniformity can also be seen in the broad excitatory tuning of the OR22a to the odor set tested (PELZ et al., 2006; Figure 24A) which leads to similar voltage changes and therefore to a similar activation pattern of the voltage gated chloride channels. Fortunately the response decrease from the antenna to the antennal lobe is no general effect and therefore is no artifact of the imaging method. Clomeleon is capable to report chloride signals in restricted morphological areas on the antenna and in the antennal lobe. In most cases there are calcium responses to the same odors in the same glomeruli where I observed also a chloride concentration change. The two response types often occur successive during odor application (LAURENT & DAVIDOWITZ, 1994; STOPFER et al., 1997) but also purely inhibitory (WILSON et al., 2004b).

It is interesting that already the chloride response pattern of a single OR allows me to distinguish the responses to several odors even though the lateral input originating from other neuronal populations contributes to the antennal lobe responses (ROOT et al., 2008).

4.5. Modulation of the transmission by a single odor

During the cameleon control experiments with the OR22a-GAL4 flies I observed a modulatory effect induced by *methyl hexanoate*. As described in the results, *methyl hexanoate* caused a response inversion of the calcium signals (Figure 25B), i.e. the normally positive odor specific cameleon signals were reversed to negative ones. This indicates a transition from a calcium influx to an efflux. *Methyl hexanoate* is the origin of this inversion since the effect is only seen after its application and the odor itself is not affected. To explain

this, an interaction of the odor with the receptor by blocking it or changing its response properties suggests itself (TURNER & RAY, 2009). Since the chloride responses were not influenced in the same manner as the calcium ones, the interaction seems to be restricted onto the calcium currents. Also a pre-depolarization of the neurons by *methyl hexanoate* and with it an increased excitatory threshold could account for such a shifting (PELZ et al., 2006; Figure 30B). However, the effect is exclusively present in the antennal lobe and not on the antenna, neither for cameleon nor clomeleon (Figure 25). This implies that the effect is related to a modification of the lateral input within the antennal lobe and not to a direct interaction of *methyl hexanoate* with OR22a. It is possible that *methyl hexanoate* interacts with another receptor to drastically change the lateral input via connected inhibitory LNs at the presynaptic site of the OR22a OSNs (OKA et al., 2004; Figure 30C). Unfortunately, the control experiments with the OR83b-cameleon flies did not give clear results. One would expect an increase in excitation in a single or several glomeruli which then would lead to an increased activation of GABAergic LNs and in turn to a stronger presynaptic inhibitory lateral input in glomerulus DM2. None of the other imaged glomeruli showed such a response pattern change to the whole odor set which would have explained the origin of the lateral input. Of course one cannot rule out that a whole set of receptors is affected by *methyl hexanoate.* In this case the responsible glomeruli would show a response change maybe only to single odors but how this would be implemented in the receptors' properties is complicated to decipher only with imaging techniques. In addition the possibilities of conventional imaging might not be sufficient and therefore the 2-photon microscopy would help to identify the responsible glomerulus in a deeper layer of the antennal lobe (WANG et al., 2003).

An often discussed issue in imaging is the necessity of high odor concentrations to evoke clear neuronal responses. In this context the application of such high concentrations (10^{-1}) is discussed as being artificial as they potentially never occur in nature and therefore derange the olfactory system by recruiting non-olfactory neurons (KEENE et al., 2004). The concentration dependence experiments show that lower concentrations of *methyl hexanoate* (10^{-3}, 10^{-5}) already evoked a weaker modulatory effect (Figure 27). The effectiveness of these more natural odor concentrations shows the potential relevance of the phenomenon for *Drosophila* as being non-artificial. An adaption within the calcium response modulation could be observed as the range of increasing *methyl hexanoate*

concentrations still evoked the modulatory effect but not to the same extent as a direct application of the highest concentration.

Furthermore the fact that the modulation is not restricted to *methyl hexanoate* itself and can be evoked by *ethyl hexanoate* too means that not the exact compound is essential but a common chemical feature that both compounds share as the hexanoate part.

Apart from the physiological effect of *methyl hexanoate* it is crucial to identify its behavioral relevance. Without a special assay to test the impact of high concentrated *methyl hexanoate* onto the perception of other odors, it is impossible to evaluate this. A potential mechanism of odor related response modulation is the effect of *2,3-butanedione* and *1-hexanol* on the CO_2 reception in *Drosophila* (TURNER & RAY, 2009). In the mentioned example the odors block the excitation by CO_2 and therefore also block the related aversive behavior. In the case of *methyl hexanoate* it is possible that the perception of a high concentration, as it indicates an extremely rewarding food source, somehow blocks the attractive reception of other odors. One possibility would be that the lateral inhibition within or between specific glomeruli is pushed by the high concentrated *methyl hexanoate* to block attractive behavior to the other odors. Further only *methyl hexanoate* would evoke a spatiotemporal patterning in the antennal lobe which leads to attraction behavior. To test this GABA antagonists like the used PTX and CGP54626 could be applied and if the hypothesis holds true they would abolish the modulatory effect.

The behavioral outcome would be that no other odor could be as attractive as *methyl hexanoate* in this situation and therefore the other odors are negligible until the food source is exploited. And since *methyl hexanoate* is a component that occurs in the scent of many fruits, it is a good indicator of food in general.

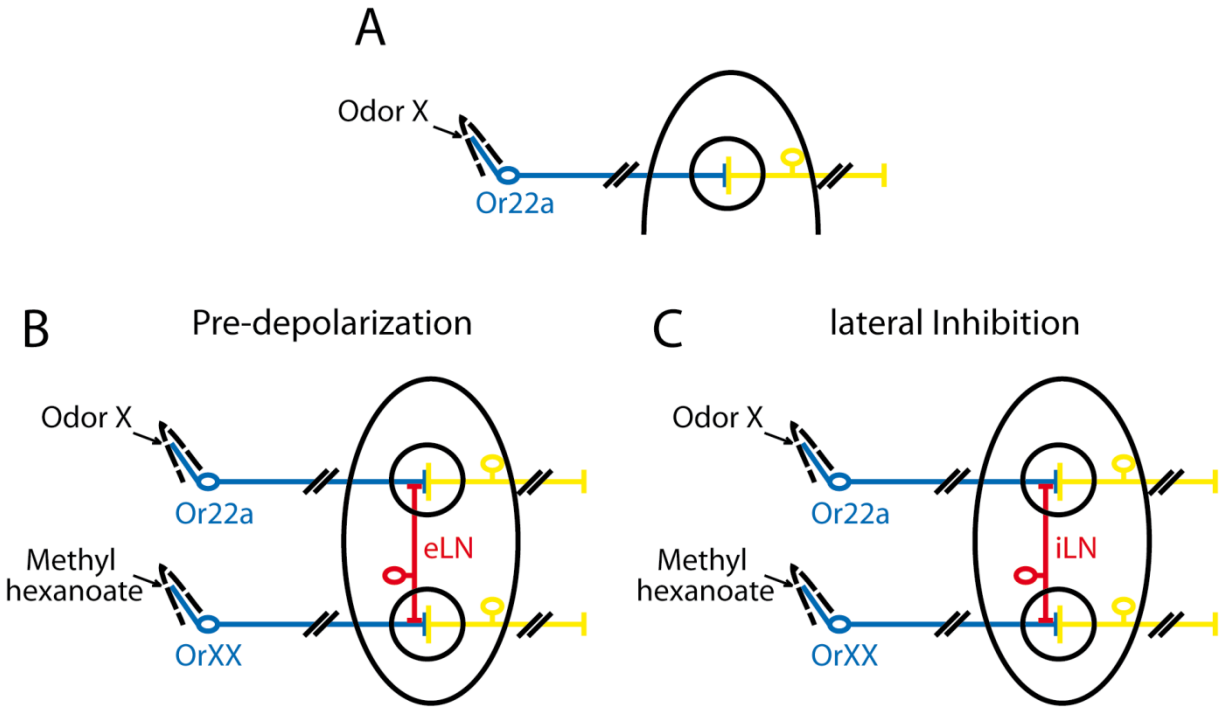

Figure 30. Potential modulatory effects of *methyl hexanoate*.
(A) Unprocessed perception of an odor by OR22a. **(B)** Modulation of the odor elicited response in OR22a-OSNs through *methyl hexanoate* evoked pre-depolarization from excitatory LNs (eLN). **(C)** Alternative modulation via lateral inhibition evoked by *methyl hexanoate* through inhibitory LNs (iLN).

4.6. An approach to a combined three-dimensional reconstruction

During my diploma thesis and especially during the mapping of spatiotemporal odor responses to identified glomeruli I often faced the problem to combine the available atlases (LAISSUE et al., 1999; COUTO et al., 2005; STOCKER et al., 1990) with my *in vivo* responses. The main problem is the gap between the atlases made from extracted and immuno-stained brains and the *in-vivo* measurements of brains that were still fixed inside the head capsule. The immuno staining has undeniable advantages as a perfect neuropil staining and the possibility to scan a brain from every possible angle. In addition the *in vivo* confocal stacks created of GAL4 lines using the 2-photon microscope have the advantage of a natural positioning inside the head and exactly the same point of view as during the imaging. With the help of the GAL4:UAS system in the immuno staining it is possible to stain the identical neurons as the ones measured *in vivo*. Since the GAL4 sequence is combined with a tissue specific driver it is always expressed in the identical neurons and with it the according UAS

driven fluorophore. After scanning the two brains one can easily identify all glomeruli in the immunostained brain due to the neuropil marker, the anti-nc82 staining. In addition one can see the glomeruli that are targeted by neurons expressing the GAL4 since they are double labeled with anti-GFP against the fluorophore. Next the glomeruli identified in the immuno-stained brain are compared with the *in vivo* ones in the fly and therefore the spatiotemporal response patterns can be easily assigned. Without the immuno-staining support it is sometimes difficult to identify glomeruli *in vivo* since the surrounding glomeruli as a reference point are not visible.

4.7. Outlook

The first important application of clomeleon will be a combination with electrophysiological techniques. This is necessary to correlate the measured chloride mediated inhibition with an actual spike frequency decrease or hyperpolarization as it has already been done for cameleon (PELZ et al., 2006). If this holds true it will be another prove of evidence that clomeleon is monitoring neuronal inhibitions.

Furthermore a combination of clomeleon imaging with behavioral assays is required to proof the potential repellent effect of odors evoking strong chloride responses.

In addition to these behavioral experiments it will be interesting to test if other odors which are known to be the best ligands for specific ORs evoke a similar signal modulation as *methyl hexanoate*.

Also it would be interesting to examine if LNs receive inhibitory input even though it is unclear if this input would originate from GABAergic PNs or from the LNs themselves. Since LNs do express GABA receptors it is obvious that they receive lateral inhibitory input (OKADA et al., 2009).

The ultimate goal is the characterization of molecular receptive ranges of every population of OSNs expressing a particular OR regarding excitation as well as inhibition. With this knowledge and the deciphered network of LNs it would be possible to predict the glomerular response pattern evoked by a single odor just by evaluating its chemical structure. From that point one could also determine the response pattern transmitted to the PNs and finally the behavioral outcome of an odor without a priori testing. An even more exclusive application

would be the possibility to determine the realistic behavioral effect of odor mixtures by integrating the information imaged for the single components.

The used conventional imaging technique allows only to functional characterize the dorsal layer of the antennal lobe. With the 2-photon microscope it will be possible to image the GAL4 lines OR83b and GH146 in deeper layers and therefore complete the glomerular odor response pattern information (WANG et al., 2003).

Clomeleon is tested to work in mice brains as well where it should detect synaptic inhibition (BERGLUND, et al., 2006; BERGLUND, et al., 2008) like in flies. This shows the diversified possibilities regarding the application of clomeleon across different species. Thus its application should also be useful in other insect species or neuronal systems apart from olfaction wherever inhibition needs to be visualized and characterized.

5. Acknowledgements

I want to thank Dr. Silke Sachse for introducing me to olfaction in the first place and supporting my work on every level.

Further I thank Prof. Dr. Bill S. Hansson for giving me the opportunity to accomplish my work at the Max-Planck-Institute for Chemical Ecology.

Especially I want to thank Antonia Strutz for the 2-photon work as well as Regina Stieber, Ronny Schäfer, Andy Sombke, Jeanine Linz, Anja Reinert, Silke Trautheim and the complete evolutionary neuroethology group in Jena for their help, the discussions and for making the work in the institute such enjoyable. For the support on the statistical interpretation of my data I want to thank Sonja Bisch-Knaden.

For the introduction into neurophysiology and dissection techniques I received from Susanne Neupert and Reinhard Predel I want to thank them.

Finally I thank Franzi and my parents for their support at all times during my thesis.

6. References

ADAMS et al., M. D. (2000). The Genome Sequence of *Drosophila melanogaster*. *Science, **287***:2185-2195.

BARGMANN, C. I. (2006). Comparative chemosensation from receptors to ecology. *Nature, **444***:295-301.

BAZHENOV, M., STOPFER, M., RABINOVICH, M., ABARBANEL, D. I., SEJNOWSKI, T. J., & LAURENT, G. (2001). Model of Cellular and Network Mechanisms for Odor-Evoked Temporal Patterning in the Locust Antennal Lobe. *Neuron, **30**:*569-581.

BENTON, R., SACHSE, S., MICHNICK, S. W., & VOSSHALL, L. B. (2006). A typical Membrane Topology and Heteromeric Function of Drosophila Odorant Receptors In Vivo. *PLOS, **4*** **(2)**:240-257.

BERDNIK, D., FAN, A. P., POTTER, C. J., & LUO, L. (2008). MicroRNA Processing Pathway Regulates Olfactory Neuron Morphogenesis. *Current Biology, **18***:1754-1759.

BERGLUND, K., SCHLEICH, W., KRIEGER, P., LOO, L. S., WANG, D., CANT, N. B., FENG, G., AUGUSTINE, G. J., KUNER, T. (2006). Imaging synaptic inhibition in transgenic mice expressing the chloride indicator, Clomeleon. *Brain Cell Biology, **35***:207-228.

BERGLUND, K., SCHLEICH, W., WANG, H., FENG, G., HALL, W. C., KUNER, T., AUGUSTINE, G. J. (2008). Imaging synaptic inhibition throughout the brain via genetically targeted Clomeleon. *Brain Cell Biology, **36***:101-118.

BICKER, G. (1999). Histochemistry of Classical Neurotransmitters in Antennal Lobes and Mushroom Bodies of the Honeybee. *Microsc Res Tech, **45***:174-183.

BRAND, A. H., & PERRIMON, N. (1993). Targeted gene expression as a means of altering cell fates and generating dominant phenotypes. *Development, **118***:401-415.

BRIEGER, G., & BUTTERWORTH, F. M. (1970). *Drosophila melanogaster*: Identity of Male Lipid in Reproductive System. *Science, **167***:1262.

BUCK, L., & AXEL, R. (1991). A Novel Multigene Family May Encode Odorant Receptors: A Molecular Basis for Odor Recognition. *Cell, **65***:175-187.

BUTTERWORTH, F. M. (1969). Lipids of *Drosophila*: A Newly Detected Lipid in the Male. *Science, **163***:1356-1357.

CASTLE, W. E. (1906). Inbreeding, Cross-Breeding and Sterility in *Drosophila*. *Science, **23*** **(578)**:153.

CLYNE, P. J., WARR, C. G., FREEMAN, M. R., LESSING, D., KIM, J., & CARLSON, J. R. (1999). A Novel Family of Divergent Seven-Transmembrane Proteins: Candidate Odorant Receptors in *Drosophila*. *Neuron, **22***:327-338.

COUTO, A., ALENIUS, M., & DICKSON, B. J. (2005). Molecular, Anatomical, and Functional Organization of the *Drosophila* Olfactory System. *Current Biology, **15***:1535-1547.

DACKS, A. M., GREEN, D. S., ROOT, C. M., NIGHORN, A. J., & WANG, J. W. (2009). Serotonin Modulates Olfactory Processing in the Antennal Lobe of *Drosophila*. *J Neurogenetics,* ***23***:366-377.

de BRUYNE, M., CLYNE, P. J., & CARLSON, J. R. (1999). Odor Coding in a Model Olfactory Organ: The *Drosophila* Maxillary Palp. *J Neurosci,* ***19*** **(11)**:4520-4532.

de BRUYNE, M., FOSTER, K., & CARLSON, J. R. (2001). Odor Coding in the *Drosophila* Antenna. *Neuron,* ***30***:537-552.

DOBRITSA, A. A., van der GOES van NATERS, W., WARR, C. G., STEINBRECHT, R. A., CARLSON, J. R. (2003). Integrating the Molecular and Cellular Basis of Odor Coding in the *Drosophila* Antenna. *Neuron,* ***37***:827-841.

DUCHAMP-VIRET, P., DUCHAMP, A., & CHAPUT, M. A. (2003). Single olfactory sensory neurons simultaneously integrate the components of an odour mixture. *Eur J Neurosci,* ***18*** **(10)**:2690-2696.

DUEBEL, J., HAVERKAMP, S., SCHLEICH, W., FENG, G., AUGUSTINE, G. J., KUNER, T., EULER, T. (2006). Two-Photon Imaging Reveals Somatodendritic Chloride Gradient in Retinal ON-Type Bipolar Cells Expressing the Biosensor Clomeleon. *Neuron,* ***49***:81-94.

EISTHEN, H. L. (2002). Why Are Olfactory Systems of Different Animals So Similar? *Brain Behav Evol,* ***59***:273-293.

ESTES, P. S., ROOS, J., van der BLIEK, A., KELLY, R. B., KRISHNAN, K. S., RAMASWAMI, M. (1996). Traffic of dynamin within individual *Drosophila* synaptic boutons relative to compartment-specific markers. *J Neurosci*, **16**:5443-5456.

FIALA, A., & SPALL, T. (2003). In Vivo Calcium Imaging of Brain Activity in *Drosophila* by Transgenic Cameleon Expression. *Sci. STKE,* ***174***:PL6.

FIALA, A., SPALL, T., DIEGELMANN, S., ELSERMANN, B., SACHSE, S., DEVAUD, J.-M., BUCHNER, E., GALIZIA, C. G. (2002). Genetically Expressed Cameleon in *Drosophila melanogaster* Is Used to Visualize Olfactory Information in Projection Neurons. *Current Biology,* ***12***:1877-1884.

FISHILEVICH, E., & VOSSHALL, L. B. (2005). Genetic and Functional Subdivision of the *Drosophila* Antennal Lobe. *Current Biology,* ***15***:1548-1553.

FRIEDRICH, R. W., & LAURENT, G. (2001). Dynamic Optimization of Odor Representations by Slow Temporal Patterning of Mitral Cell Activity. *Science,* ***291***:889-894.

GAO, Q., YUAN, B., & CHESS, A. (2000). Convergent projections of *Drosophila* olfactory neurons to specific glomeruli in the antennal lobe. *Nature Neurosci,* ***3*** **(8)**:780-785.

GOLDMAN, A. L., van der GOES van NATERS, W. V., LESSING, D., WARR, C. G., & CARLSON, J. R. (2005). Coexpression of Two Functional Odor Receptors in One Neuron. *Neuron,* ***45***:661-666.

HALLEM, E. A., & CARLSON, J. R. (2006). Coding of Odorsby a ReceptorRepertoire. *Cell,* ***125***:143-160.

HALLEM, E. A., HO, M. G., & CARLSON, J. R. (2004). The Molecular Basis of Odor Coding in the *Drosophila* Antenna. *Cell,* ***117***:965-979.

HAMASAKA, Y., WEGENER, C., & NÄSSEL, D. R. (2005). GABA Modulates *Drosophila* Circadian Clock Neurons via GABAB Receptors and Decreases in Calcium. *J Neurobiology,* ***65*** **(3)**:225-240.

HARRISON, J. B., CHEN, H. H., SATTELLE, E., BARKER, P. J., HUSKINSSON, N. S., RAUH, J. J., BAI, D., SATTELLE, D. B. (1996). Immunocytochemical mapping of a C-terminus anti-peptide antibody to the GABA receptor subunit, RDL in the nervous system of *Drosophila melanogaster*. *Cell Tiss Res*, **284**:269-278.

HAVERKAMP, S., WÄSSLE, H., DUEBEL, J., KUNER, T., AUGUSTINE, G. J., FENG, G., EULER, T. (2005). The Primordial, Blue-Cone Color System of the Mouse Retina. *J Neurosci,* ***25*** **(22)**:5438-5445.

HILDEBRAND, J. G., & SHEPERD, G. M. (1997). MECHANISMS OF OLFACTORY DISCRIMINATION: Converging Evidence for Common Principles Across Phyla. *Annu Rev Neurosci,* ***20***:595-631.

HOSKINS, S. G., HOMBERG, U., KINGAN, T. G., CHRISTENSEN, T. A., & HILDEBRAND, J. G. (1986). Immunocytochemistry of GABA in the antennal lobes of the sphinx moth Manduca sexta. *Cell Tiss Res*, **244**:243-252.

ITO, K., SASS, H., URBAN, J., HOFBAUER, A., & SCHNEUWLY, S. (1997). GAL4-responsive UAS-tau as a tool for studying the anatomy and development of the *Drosophila* central nervous system. *Cell Tiss Res,* ***290***:1-10.

JEFFERIS, G. S., MARIN, E. C., STOCKER, R. F., & LUO, L. (2001). Target neuron prespecifcation in the olfactorymap of *Drosophila*. *Nature,* ***414***:204-208.

KACZOROWSKI, C. C., DISTERHOFT, J., & SPRUSTON, N. (2007). Stability and plasticity of intrinsic membrane properties in hippocampal CA1 pyramidal neurons: effects of internal anions. *J Physiol,* ***578*** **(3)**:799-818.

KAUPMANN, K., HUGGEL, K., HEID, J., FLOR, P. J., BISCHOFF, S., MICKEL, S. J., McMASTER, G., ANGST, C., BITTIGER H., FROESTL, W., BETTLER, B. (1997). Expression cloning of GABAB receptors uncovers similarity to metabotropic glutamate receptors. *Nature,* ***386***:239-246.

KEENE, A. C., STRATMANN, M., KELLER, A., PERRAT, P. N., VOSSHALL, L. B., & WADDELL, S. (2004). Diverse Odor-Conditioned Memories Require Uniquely Timed Dorsal Paired Medial Neuron Output. *Neuron*, **44**:521-533.

KUNER, T., & AUGUSTINE, G. J. (2000). A Genetically Encoded Ratiometric Neurotechnique Indicator for Chloride: Capturing Chloride Transients in Cultured Hippocampal Neurons. *Neuron,* ***27***:447-459.

LAISSUE, P. P., REITER, C., HIESINGER, P. R., HALTER, S., FISCHBACH, K. F., & STOCKER, R. F. (1999). Three-Dimensional Reconstruction of the Antennal Lobe in *Drosophila melanogaster*. *J Comp Neurol,* ***405***:543-552.

LARSSON, M. C., DOMINGOS, A. I., JONES, W. D., CHIAPPE, M. E., AMREIN, H., & VOSSHALL, L. B. (2004). OR83b Encodes a Broadly Expressed Odorant Receptor Essential for *Drosophila* Olfaction. *Neuron,* ***43***:703-714.

LAURENT, G., & DAVIDOWITZ, H. (1994). Encoding of Olfactory Information with Oscillating Neural Assemblies. *Science,* ***265***:1872-1875.

LEITCH, B., & LAURENT, G. (1996). GABAergic Synapses in the Antenna1 Lobe and Mushroom Body of the Locust Olfactory System. *J Comp Neurol,* ***372***:487-514.

MALUN, D. (1991). Synaptic relationships between GABA-immunoreaetive neurons and an identified uniglomerular projection neuron in the antennal lobe of *Periplaneta americana*: a double-labeling electron microscopic study. *Histochemsitry,* ***96***:197-207.

MIESENBÖCK, G., de ANGELIS, D. A., & ROTHMAN, J. E. (2001). Visualizing secretion and synaptic transmission with pH-sensitive green fluorescent proteins. *Nature,* ***394***:192-195.

MIYAWAKI, A., LLOPIS, J., HEIM, R., McCAFFERY, J. M., ADAMS, J. A., IKURA, M., TSIEN, R. Y. (1997). Fluorescent indicators for Ca^{2+} based on green fluorescent proteins and calmodulin. *Nature,* ***388***:882-887.

MOMBAERTS, P. (1999). Seven-Transmembrane Proteins as Odorant and Chemosensory Receptors. *Science,* ***286***:707-711.

NEUHAUS, E. M., GISSELMANN, G., ZHANG, W., DOOLEY, R., STÖRTKUHL, K., & HATT, H. (2005). Odorant receptor heterodimerization in the olfactory system of *Drosophila melanogaster*. *Nat Neurosci,* ***8*** **(1)**:15-17.

NG, M., ROORDA, R. D., LIMA, S. Q., ZEMELMAN, B. V., MORCILLO, P., & MIESENBÖCK, G. (2002). Transmission of Olfactory Information between Three Populations of Neurons in the Antennal Lobe of the Fly. *Neuron,* ***36***:463-474.

OKA, Y., OMURA, M., KATAOKA, H., & TOUHARA, K. (2004). Olfactory receptor antagonism between odorants. *EMBO J,* ***23***:120-126.

OKADA, R., AWASAKI, T., ITO, K. (2009). Gamma-Aminobutyric Acid (GABA)-Mediated Neural Connections in the *Drosophila* Antennal Lobe. *J Comp Neurol,* ***514***:74-91.

OLSEN, S. R., & WILSON, R. I. (2008). Lateral presynaptic inhibition mediates gain control in an olfactory circuit. *Nature,* ***452***:956-960.

PELZ, D., ROESKE, T., SYED, Z., de BRUYNE, M., GALIZIA, C. G. (2006). The Molecular Receptive Range of an Olfactory Receptor in vivo (*Drosophila melanogaster* OR22a). *J Neurobiology,* ***66*** **(14)**:1544-1563.

POND, B. B., BERGLUND, K., KUNER, T., FENG, G., AUGUSTINE, G. J., & SCHWARTZ-BLOOM, R. D. (2006). The Chloride Transporter Na^{+} -K^{+} -Cl^{-} Cotransporter Isoform-1 Contributes to Intracellular Chloride Increases after *In Vitro* Ischemia. *J Neurosci,* ***26*** **(5)**:1396-1406.

POPHOF, B. (2004). Pheromone-binding Proteins Contribute to the Activation of Olfactory Receptor Neurons in the Silkmoths *Antheraea polyphemus* and *Bombyx mori*. *Chem Senses,* ***29*** **(2)**:117-125.

PYTHON, F., & STOCKER, R. F. (2002). Immunoreactivity Against Choline Acetyltransferase, -Aminobutyric Acid, Histamine, Octopamine, and Serotonin in the Larval Chemosensory System of *Drosophila melanogaster*. *J Comp Neurol,* ***453***:157-167.

ROBERTSON, H. M., WARR, C. G., & CARLSON, J. R. (2003). Molecular evolution of the insect chemoreceptor gene superfamily in *Drosophila melanogaster*. *PNAS,* ***100*** **(2)**:14537–14542.

ROOT, C. M., MASUYAMA, K., GREEN, D. S., ENELL, L. E., NÄSSEL, D. R., LEE, C.-H., WANG, J. W. (2008). A Presynaptic Gain Control Mechanism Fine-Tunes Olfactory Behavior. *Neuron,* ***59*** **(2)**:311-321.

SCHMIDT-RHAESA, A. (2007). The Evolution of ORGAN SYSTEMS, 7. Sensory Organs. Oxford University Press.

SHANBHAG, S. R., MÜLLER, B., & STEINBRECHT, R. A. (1999). Atlas of olfactory organs of *Drosophila melanogaster* 1. Types, external organization, innervation and distribution of olfactory sensilla. *Int J Insect Morphol Embryol,* ***28***:377-397.

SHANG, Y., CLARIDGE-CHANG, A., SJULSON, L., PYPAERT, M., & MIESENBÖCK, G. (2007). Excitatory Local Circuits and Their Implications for Olfactory Processing in the Fly Antennal Lobe. *Cell,* ***128***:601-612.

SHIROKOVA, E., SCHMIEDEBERG, K., BEDNER, P., NIESSEN, H., WILLECKE, K., RAGUSE, J.-D., MEYERHOF, W., KRAUTWURST, D. (2005). Identification of Specific Ligands for Orphan Olfactory Receptors. *J Biol Chem,* ***280*** **(12)**:11807-11815.

SILBERING, A. F., OKADA, R., ITO, K., & GALIZIA, C. G. (2008). Olfactory Information Processing in the *Drosophila* Antennal Lobe: Anything Goes? *J Neurosci,* ***28*** **(49)**:13075-13087.

SINAKEVITCH, I., & STRAUSFELD, N. J. (2006). Comparison of Octopamine-Like Immunoreactivity in the Brains of the Fruit Fly and Blow Fly. *J Comp Neurol,* ***494***:460-475.

STENSMYR, M. C., GIORDANO, E., BALLOI, A., ANGIOY, A.-M., & HANSSON, B. S. (2003). Novel natural ligands for *Drosophila* olfactory receptor neurones. *J Exp Biol,* ***206***:715-724.

STOCKER, R. F. (1994). The organization of the chemosensory system in *Drosophila melanogaster*: a rewiew. *Cell Tiss Res,* ***275***:3-26.

STOCKER, R. F., HEIMBECK, G., GENDRE, N., & de BELLE, J. S. (1997). Neuroblast Ablation in *Drosophila* P[GAL4] Lines Reveals Origins of Olfactory Interneurons. *J Neurobiol, 32*, pp. 443-456.

STOCKER, R. F., LIENHARD, M. C., BORST, A., & FISCHBACH, K. F. (1990). Neuronal architecture of the antennal lobe in *Drosophila melanogaster*. *Cell and Tissue Research,* ***262***:9-34.

STOPFER, M., BHAGAVAN, S., SMITH, B. H., LAURENT, G. (1997). Impaired odourdiscrimination on desynchronization of odour-encoding neural assemblies. *Nature,* ***390***:70-74.

STOPFER, M. (2005). Olfactory Coding: Inhibition Reshapes Odor Responses. *Current Biology, **15*** **(24)**:996-998.

TURNER, S. L., & RAY, A. (2009). Modification of CO2 avoidance behaviour in *Drosophila* by inhibitory odorants. *Nature, **461*** **(7261)**:277-281.

VOSSHALL, L. B., & STOCKER, R. F. (2007). Molecular Architecture of Smell and Taste in *Drosophila*. *Annu Rev Neurosci, **30***:505-533.

VOSSHALL, L. B., AMREIN, H., MOROZOV, P. S., RZHETSKY, A., & RICHARD, A. (1999). A Spatial Map of Olfactory Receptor Expression in the *Drosophila* Antenna. *Cell, **96***:725-736.

VOSSHALL, L. B., WONG, A. M., & AXEL, R. (2000). An Olfactory Sensory Map in the Fly Brain. *Cell, **102***:147-159.

WANG, J. W., WONG, A. M., FLORES, J., VOSSHALL, L. B., & AXEL, R. (2003). Two-Photon Calcium Imaging Reveals an Odor-Evoked Map of Activity in the Fly Brain. *Cell, **112***:271-282.

WANG, L., & ANDERSON, D. J. (2010). Identification of an aggression-promoting pheromone and its receptor neurons in *Drosophila*. *Nature, **463***:227-232.

WÄSSLE, H., PULLER, C., MÜLLER, F., & HAVERKAMP, S. (2009). Cone contacts, mosaics, and territories of bipolar cells in the mouse retina. *J Neurosci, **29*** **(1)**:106-117.

WICHER, D., WALTHER, C., & WICHER, C. (2001). Non-synaptic ion channels in insects - basic properties of currents and their modulation in neurons and skeletal muscles. *Prog Neurobiol, **64***:431-525.

WILSON, R. I., & LAURENT, G. (2005). Role of GABAergic Inhibition in Shaping Odor-Evoked Spatiotemporal Patterns in the *Drosophila* Antennal Lobe. *J Neuroscience, **25*** **(40)**:9069-9079.

WILSON, R. I., TURNER, G. C., & LAURENT, G. (2004b). Transformation of Olfactory Representations in the *Drosophila* Antennal Lobe. *Science, **303***:366-370.

7. Declaration of original authorship

I hereby declare that the work submitted is my own and that all passages and ideas that are not mine have been fully and properly acknowledged.

Jena, 02/22/2010 ……..

8. Abbreviations

AL…	antennal lobe
ANI…	*anisole*
APT…	antenno protocerebral tract
BEA…	*benzaldehyde*
BP…	band pass filter
CCD…	charged coupled device
CGP54626…	P-(3-aminopropyl)-P-diethoxymethylphosphinic acid
CVA…	*11-cis vaccenyl acetate*
D…	dorsal (glomeruli)
DCRX…	dichroic mirror
DL…	dorso-lateral (glomeruli)
DM…	dorso-medial (glomeruli)
DP…	dorso-posterior (glomeruli)
eCFP…	enhanced Cyan Fluorescent Protein
EHB…	*ethyl-3-hydroxy butyrate*
EHE…	*ethyl hexanoate*
eLN…	excitatory local interneuron (cholinergic)
ETB…	*ethyl benzoate*
eYFP…	enhanced Yellow Fluorescent Protein
FRET…	Fluorescence Resonance Electron Transport
G-CaMP…	a genetically encoded calcium indicator (GECI)
GABA…	γ-aminobutyric acid
GAL4…	yeast specific transcription factor
GFP…	Green Fluorescent Protein
GH146…	PN specific GAL4 driver line
GR…	gustatory receptor
GVL…	*γ-valerolactone*
HEX…	*1-hexanol*
HQ…	emission filter
iLN…	inhibitory local interneuron (GABAergic)

ISI…	interstimulus interval
ISO…	*isoamyl acetate*
lAPT…	lateral antennoprotocerebral tract
LN…	local interneuron
M13…	calmodulin binding protein
mAPT…	medial antennoprotocerebral tract
MB…	mushroom body
MHE…	*methyl hexanoate*
mlAPT…	mediolateral antennoprotocerebral tract
nc82…	monoclonal antibody against *bruchpilot*
OBP…	odorant binding protein
OR…	olfactory receptor
OSN…	olfactory sensory neuron
PB…	phosphate buffer
PBS…	phosphate buffered saline
PBST…	PBS + Triton
PBST-NGS…	PBST + normal goat serum
PEC…	*pentyl acetate*
Ped…	pedunculus
PFA…	paraformaldehyde
PN…	projection neuron
PTX…	picrotoxin
RNA…	ribonucleic acid
SOG…	suboesophageal ganglion
SP…	short pass filter
UAS…	upstream activating sequence
VA…	ventro-anterior (glomeruli)
VL…	ventro-lateral (glomeruli)
VM…	ventro-median (glomeruli)

9. Appendix

Immunostaining protocol (by Jeanine Linz)

1st day

Anesthetization of flies under CO_2 for circa 10 minutes on -20°C

Fix flies in 1ml fix solution (500µl Phosphate Buffer (PB, 0.2M), 500µl Paraformaldehyde (PFA, 8%) + 200µl Triton x-100).

Mix 3 hours at 4°C on a rocking shaker.

Replace fix solution with wash solution (100ml Phosphate Buffered Saline (PBS) + 200µl Triton x-100 (PBST)).

Rinse quickly for 2 times.

Wash over night with 1ml PBST at 4°C on a rocking shaker.

2nd day

Dissect the brains in PBST and remove the trachea. Collect them in 500µl blocking solution (PBST + 5% Normal Goat Serum (PBST-NGS)) on ice.

Incubate the brains for 1 hour at room temperature.

Exchange blocking solution with 200µl primary antibody solution (185µl PBST-NGS, 17µl mouse α-nc82, 0.5µl rabbit α-GFP). Wrap the eppendorf tube in aluminum foil.

Incubate for 2-3 days at 4°C on a rocking shaker in darkness.

4th/5th day

Replace primary antibody solution with wash solution (see above).

Rinse 3 times for 20 minutes at room temperature on a rocking shaker in darkness (aluminum foil).

Exchange wash solution with 200µl secondary antibody solution (200µl PBST-NGS, 1µl α-mouse alexa 546, 1µl α-rabbit alexa 488). Wrap the eppendorf tube in aluminum foil.

Incubate for 2-3 days at 4°C on a rocking shaker in darkness.

6th/7th day

Replace secondary antibody solution with wash solution (see above).

Rinse 3 times for 20 minutes at room temperature on a rocking shaker in darkness (aluminum foil).

Remove PBST and add 400µl Vectashield and store at 4°C till mounting.